

Inelastic heavy quarkonium photoproduction in ultrarelativistic heavy-ion collisions

Zhi-Lei Ma,^{1,2} Zhun Lu,³ and Li Zhang^{2,*}

¹*Department of Physics, Yunnan University, Kunming 650091, China*

²*Department of Astronomy, Key Laboratory of Astroparticle Physics
of Yunnan Province, Yunnan University, Kunming 650091, China*

³*School of Physics, Southeast University, Nanjing 211189, China*

(Dated: March 24, 2022)

The inelastic charmonium (J/ψ , $\psi(2S)$, η_c , h_c and χ_{cJ}) and bottomonium ($\Upsilon(nS)$, η_b , h_b , and χ_{bJ}) photoproductions in ultrarelativistic heavy-ion collisions at LHC energies are studied, where the fragmentation processes are included. Based on the factorization formalism of non-relativistic QCD, an exact treatment is developed, which can weight the contribution from different channels and recovers the Weizsäcker-Williams approximation (WWA) near the region $Q^2 \sim 0$. The relevant kinematical relations are also achieved. We present a comprehensive analysis for the properties of WWA in heavy-ion collisions, and discuss the contribution of inelastic photoproduction processes to the heavy quarkonium production. The Q^2 -, y -, \sqrt{s} -, and p_T -dependent cross sections, and the total cross sections are estimated. It is shown that the inelastic photoproduction and fragmentation processes can provide the evident modification to the heavy quarkonium production in p - p and Pb - Pb collisions at LHC energies, where the ultra-incoherent photon emission plays a very important role. Moreover, the WWA is only effective in very restricted domains, and the exact treatment can naturally avoid double counting and WWA errors.

I. INTRODUCTION

The study of heavy quarkonium has yielded valuable insight into the nature of the strong interaction, $Q\bar{Q}$ bound states have provided useful laboratories for probing both perturbative and nonperturbative aspects of QCD. During the last years the study of the heavy vector meson produced by photon-induced interactions at hadronic colliders has been strongly motivated by the possibility of constraining the dynamics of the strong interactions at high energies [1–6], it sheds light on the low- x physics and helps to constraint the nuclear parton distributions [7–11]. It is well known that this types of mechanism can be theoretically studied using the Weizsäcker-Williams approximation (WWA) [12–14]. The central idea of WWA is that the moving electromagnetic field of charged particles can be treated as a flux of photons. In an ultrarelativistic ion collider, theses photons can interact with target nucleus in the opposing beam (photoproduction) or with the photons of the opposing beam (two-photon reactions). At the CERN Large Hadron Collider (LHC) energies, the intense heavy-ion beams represent a prolific source of quasireal photons, hence it enables extensive studies of photon-induced physics. In the calculations, an important function is the photon flux function, which has different forms for different charged sources.

Although the great success has been achieved, the properties of WWA in heavy quarkonium photoproduction are rarely noticed. WWA is usually employed to the processes which are actually inapplicable, and the imprecise statements pertaining to the essence of WWA were

given [15–31]. For instance, the WWA is usually adopted in electroproduction reactions or elastic processes, where virtuality Q^2 of the photon γ^* is very small, controlled by the electron mass m_e or coherence condition. However when the WWA is used in hadronic collisions it is the nucleus mass m_N which controls the photon virtuality and it is not obvious that the WWA is still valid. Particularly in the case of ultrarelativistic heavy-ion collisions at LHC energies, the influence of WWA becomes significant to the accuracy of photoproduction processes, since photon flux function scale as $f_\gamma \propto Z^2 \ln \sqrt{s}/m$, the collision energy \sqrt{s} and the square of nuclear charge Z^2 are the very large enhancement factors to the cross sections. Thus, heavy-ion collisions have a considerable flux advantage over the proton. For these reasons, it is necessary to present a comprehensive analysis of WWA in heavy-ion collisions, and to estimate the important inaccuracies appeared in its application.

On the other hand, there are two kinds of photon emission mechanisms on the side of photon emitter [32]: coherent-photon emission (coh.) and incoherent-photon emission (incoh.). In the first type, the virtual photons are emitted coherently by the whole nucleus which remains intact after photons radiated. In the second type, the virtual photons are emitted incoherently by the individual constituents (protons or quarks) inside nucleus, and the nucleus will dissociate after photons radiated. For convenience, in the second type we further denote the process in which photons emitted from protons inside nucleus as ordinary-incoherent photon emission (OIC), and denote that from quarks inside nucleus as ultra-incoherent photon emission (UIC). To avoid confusion, the terminology “elastic” and “inelastic” describe the case of whether the target nucleus remains intact or is allowed to break up after the scattering with photons. When these different channels are considered simultane-

*Electronic address: lizhang@ynu.edu.cn

ously, we have to weight the different contributions to avoid double counting. But in fact, this serious trouble is encountered in most works and brings the large fictitious contributions [16–23].

There are a lot of studies for these processes, however, the application of UIC, to our knowledge, is insufficient in heavy quarkonium photoproduction. For instance, Gonçalves presented a systematical analysis of exclusive production of vector mesons in hadronic collisions in Refs. [33–37], where the predictions for transverse momentum and rapidity distributions considering different phenomenological models were estimated. Machado et al. studied the inclusive and exclusive J/ψ , $\psi(2S)$, and Υ photoproductions in the proton-nucleus and nucleus-nucleus collisions at LHC within the color dipole formalism [38–41]. In Refs. [42–44], Klein and Nystrand studied the coherent and elastic vector meson production via photon-Pomeron and photon-meson interactions, these authors also presented a Monte Carlo simulation program, STARTlight, that calculated the cross sections for a variety of UPC final states [45]. There are also a lot of other works for heavy quarkonium photoproduction. However, the photon emission types in all of these above works are coherent, the incoherent-photon emission is neglected. Furthermore, the UIC photoproduction, which is best treated as inclusive processes, can provide additional correction to the central collisions. For instance, authors in Refs. [18–20] have investigated the inelastic dileptons, photons, and light vector mesons productions at LHC energies. These works show that the UIC photoproduction can provide the meaningful contribution to massless and light-state particles productions in the central collisions. However, the correction is not clear for heavy quarkonium due to its large mass.

According to the purposes discussed above, in present work, we consider the heavy quarkonium photoproduction in p - p and Pb - Pb collisions at LHC energies. An exact treatment is performed that recovers the WWA near the region $Q^2 \sim 0$ and can be considered as the generalization of Leptoproduction [46]. The full kinematical relations matched with the exact treatment are also obtained. We present a consistent analysis of the properties of WWA in heavy-ion collisions, and discuss the contributions of photoproduction and fragmentation processes to leading order (LO) contributions.

This paper is organized as follows. Section II presents the formalism of exact treatment for the heavy quarkonium photoproduction. Based on Martin-Ryskin method, the coherent, ordinary-incoherent, and ultra-incoherent photon emissions are considered simultaneously. In Section III, we turn the accurate formula into the WWA one near the region $Q^2 \sim 0$, and study the several widely employed photon flux functions. We present the numerical results in Section IV, the Q^2 -, y -, \sqrt{s} -, and p_T -dependent cross sections, and the total cross sections are achieved. Finally, we summarize the paper in Section V.

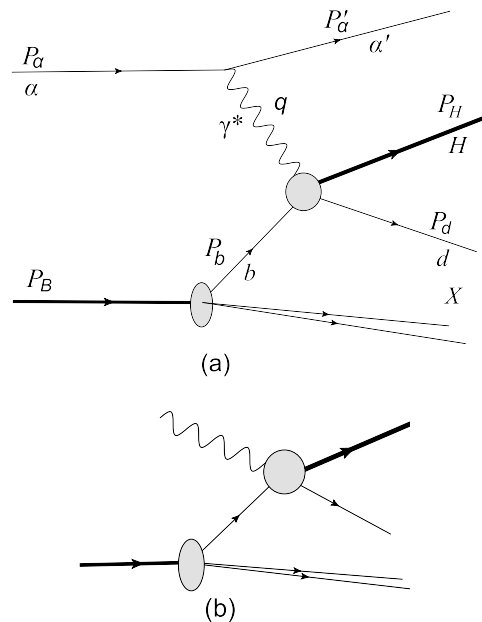


FIG. 1: (a) The general inelastic heavy quarkonium photoproduction process. The virtual photon emitted from the projectile α interacts with parton b of target nucleus B , α can be the nucleus or its charged parton (protons or quarks). (b): real photo-absorption.

II. GENERAL FORMALISM OF EXACT TREATMENT

For heavy quarkonium production and decay, the non-relativistic QCD (NRQCD) factorization scheme, which was proposed to explain the huge discrepancy between the theoretical prediction and experimental measurements of the transverse momentum distribution of J/ψ production at the Tevatron, has been a very successful scheme in many applications [47]. In this section, we employ this formalism to describe the inelastic charmonium and bottomonium photoproductions. The NRQCD formalism implies a separation of process-dependent short-distance coefficients to be studied using the perturbative theory from supposedly process-independent long-distance matrix elements (MEs) to be extracted from experiment. The relative importance of the latter can be estimated by means of velocity scaling rules, i.e., the MEs are predicted to scale with a power of the heavy-quark relative velocity v in the limit $v \ll 1$. In this way, the theoretical predictions are organized as double expansions in α_s and v . A crucial feature of this formalism is that it takes into account the $Q\bar{Q}$ Fock space, which is spanned by the states $n = {}^{2S+1}L_J^{(c)}$. In particular, this formalism predicts the existence of color-octet processes in nature by the nonperturbative emission of soft gluons. In the present paper, it is too long to list here the involved wavefunctions and the MEs of the charmonium (J/ψ , $\psi(2S)$, η_c , h_c and χ_{cJ}) and bottomonium (Υ_{nS} , χ_{bJ} , h_b , and η_b), and we summarized them in Appendix A for completeness and convenience.

A. The accurate cross section for the general inelastic photoproduction process $\alpha b \rightarrow \alpha H X$

The exact treatment for the heavy quarkonium photoproduction in heavy-ion collisions can be considered as proceeding in two steps. In the first step, the density matrix of virtual photon should be expended using the polarization operators, based on the fact that the photon radiated from the projectile is off mass shell and no longer transversely polarized. In the second step, the square of the electric form factor $D(Q^2)$ is adopted as the weighting factor (WF) to weight the different charged sources, thus we can avoid the trouble of double counting.

Through a consistent analysis of the terms neglected in going from the accurate formula of Fig. 1(a) to the WWA one, we can naturally estimate the properties of WWA in heavy-ion collisions. This actually can be performed in a general form for every reaction, in our case, for achieving the first step of exact treatment we should derive the general form of cross section for the inelastic heavy quarkonium photoproduction in Fig. 1(a),

$$d\sigma(\alpha + B \rightarrow \alpha + H + X) = \sum_b \int dx_b f_{b/B}(x_b, \mu_b^2) d\sigma(\alpha + b \rightarrow \alpha + H + d), \quad (1)$$

where $x_b = p_b/p_B$ is the momentum fraction of the massless parton b (quark or gluon) struck by the virtual photon, $f_{b/B}(x_b, \mu_b^2)$ is the distribution function of b in nucleus B ,

$$f_i^A(x_i, \mu_i^2) = R_i^A(x_i, \mu_i^2) [Z p_i(x_i, \mu_i^2) + N n_i(x_i, \mu_i^2)], \quad (2)$$

where the factorized scale is chosen as $\mu_i = \sqrt{m_H^2 + Q^2}$, $R_i(x, \mu_i^2)$ is the nuclear modification function which reflect the nuclear shadowing effect [48], Z is the proton number, $N = A - Z$ is the neutron number and A is the nucleon number. $p_i(x, \mu^2)$ and $n_i(x, \mu^2)$ are the parton distributions of the protons and neutrons [49], respectively. According to the NRQCD factorization formalism, the partonic cross section in Eq. (1) can be written as

$$d\sigma(\alpha + b \rightarrow \alpha + H + d) = \sum_n \langle \mathcal{O}_{[1,8]}^H[n] \rangle d\sigma(\alpha + b \rightarrow \alpha + Q\bar{Q}_{[1,8]} + d). \quad (3)$$

where $\langle \mathcal{O}_{[1,8]}^H[n] \rangle$ is the MEs of NRQCD.

By denoting the virtual photo-absorption amplitude as M^μ , we obtain the differential cross section in the parton level

$$d\sigma(\alpha + b \rightarrow \alpha + Q\bar{Q}_{[1,8]} + d) = \frac{4\pi e_\alpha^2 \alpha_{\text{em}}}{Q^2} \rho_{\mu\nu} M^\mu M^{*\nu} \frac{d^3 p'_\alpha}{(2\pi)^3 2E'_\alpha} \times \frac{(2\pi)^4 \delta^4(p_\alpha + p_b - p'_\alpha - k) d\Gamma}{4\sqrt{(p_\alpha \cdot p_b)^2 - m_\alpha^2 m_b^2}}, \quad (4)$$

here e_α is the charge of α , $\alpha_{\text{em}} = 1/137$ is the electromagnetic coupling constant, $E_{\alpha'}$ is the energy of α' , and Γ is a phase space volume of the produced particle system with total momentum k . Keeping in mind the process, in which photons may be emitted by various particles, we shall give a generalized density matrix of a virtual photon as follows,

$$\begin{aligned} \rho^{\mu\nu} &= \frac{1}{2Q^2} \text{Tr}[(p_\alpha + m_\alpha) \Gamma^\mu (p'_\alpha + m_\alpha) \Gamma^\nu] \\ &= \left(-g^{\mu\nu} + \frac{q^\mu q^\nu}{q^2} \right) C(Q^2) \\ &\quad - \frac{(2P_\alpha - q)^\mu (2P_\alpha - q)^\nu}{q^2} D(Q^2), \end{aligned} \quad (5)$$

where $C(Q^2)$ and $D(Q^2)$ are the general notations of form factors for α . Let us note that the $\rho^{\mu\nu}$ is non-diagonal, i.e. the virtual photons are polarized. The expression of Eq. (4) is written in such a form as to introduce naturally the terminology which is suitable for WWA. Namely, instead of speaking about the nucleus-nucleus collisions [Fig. 1(a)] one may speak about the collisions of a virtual photon with the nucleus [Fig. 1(b)].

Now we employ the accurate expression Eq. (4) to give the Q^2 - and y -dependent differential cross section for the heavy quarkonium photoproduction. It is further convenient to do the calculations in the rest frame of α , where $|\mathbf{q}| = |\mathbf{p}_{\alpha'}| = r$, $Q^2 = -q^2 = (p_\alpha - p_{\alpha'})^2 = 2m_\alpha(\sqrt{r^2 + m_\alpha^2} - m_\alpha)$, $d^3 p'_\alpha = r^2 dr d\cos\theta d\varphi$, and $y = (q \cdot p_b)/(p_\alpha \cdot p_b) = (q_0 - |\mathbf{p}_b| r \cos\theta/E_b)/m_\alpha$ (which measures the relative energy loss of α in the lab-system). By doing the following transformation,

$$d\cos\theta dr = \mathcal{J} dQ^2 dy = \left| \frac{D(r, \cos\theta)}{D(Q^2, y)} \right| dQ^2 dy, \quad (6)$$

the details of \mathcal{J} are given in Appendix B, the differential cross section in Eq. (4) can be turned into,

$$\begin{aligned} &\frac{d\sigma(\alpha + b \rightarrow \alpha + Q\bar{Q}_{[1,8]} + d)}{dQ^2 dy} \\ &= \frac{e_\alpha^2 \alpha_{\text{em}}}{4\pi Q^2} \rho_{\mu\nu} M^\mu M^{*\nu} f(s_{\alpha b}, p_{\text{CM}}, \hat{s}, \hat{p}_{\text{CM}}) \\ &\quad \times \frac{(2\pi)^4 \delta^4(p_\alpha + p_b - p'_\alpha - k) d\Gamma}{4\hat{p}_{\text{CM}} \sqrt{\hat{s}}}, \end{aligned} \quad (7)$$

and

$$\begin{aligned} &f(s_{\alpha b}, p_{\text{CM}}, \hat{s}, \hat{p}_{\text{CM}}) \\ &= \frac{\hat{p}_{\text{CM}} \sqrt{\hat{s}}}{p_{\text{CM}} \sqrt{s_{\alpha b}}} \frac{s_{\alpha b} - m_\alpha^2 - m_b^2}{\sqrt{(s_{\alpha b} - m_\alpha^2 - m_b^2)^2 - 4m_\alpha^2 m_b^2}}. \end{aligned} \quad (8)$$

where $s_{\alpha b} = (p_\alpha + p_b)^2$ and $\hat{s} = (q + p_b)^2$ are the energy square in the αb and $\gamma^* b$ CM frames, respectively. p_{CM} and \hat{p}_{CM} are the momenta in the corresponding CM frames. The details are summarized in Appendix B.

After integrating over the phase space volume Γ of the produced system of particles, the following quantity will be included in the result Eq. (7):

$$W^{\mu\nu} = \frac{1}{2} \int M^{*\nu} M^\mu (2\pi)^4 \delta^4(p_\alpha + p_b - p'_\alpha - k) d\Gamma, \quad (9)$$

where $W^{\mu\nu}$ is the absorptive part of the γb amplitude [Fig. 1(b)], which is connected with the cross section in the usual way. The tensors according to which $W^{\mu\nu}$ is expanded, can be constructed only from the q , p_b and $g^{\mu\nu}$ tensor. In order to take into account gauge invariance: $q^\mu W^{\mu\nu} = q^\nu W^{\mu\nu} = 0$, it is convenient to use the following transverse and longitudinal polarization operators [50]

$$\begin{aligned} \epsilon_T^{\mu\nu} &= -g^{\mu\nu} + \frac{(q^\mu p_b^\nu + p_b^\mu q^\nu)}{q \cdot p_b} - \frac{p_b^\mu p_b^\nu q^2}{(q \cdot p_b)^2}, \\ \epsilon_L^{\mu\nu} &= \frac{1}{q^2} \left(q^\mu - p^\mu \frac{q^2}{q \cdot p_b} \right) \left(q^\nu - p^\nu \frac{q^2}{q \cdot p_b} \right), \end{aligned} \quad (10)$$

which satisfy the relations: $q_\mu \epsilon_T^{\mu\nu} = q_\mu \epsilon_L^{\mu\nu} = 0$, $\epsilon_{T\mu}^\mu = -2$, and $\epsilon_{L\mu}^\mu = -1$. Furthermore,

$$\epsilon^{\mu\nu} = \epsilon_T^{\mu\nu} + \epsilon_L^{\mu\nu} = -g^{\mu\nu} + \frac{q^\mu q^\nu}{q^2} \quad (11)$$

is the polarization tensor of an unpolarized spin-one boson with mass q^2 . Having expended $W^{\mu\nu}$ in these tensors, we achieve

$$W^{\mu\nu} = \epsilon_T^{\mu\nu} W_T(Q^2, q \cdot p_b) + \epsilon_L^{\mu\nu} W_L(Q^2, q \cdot p_b). \quad (12)$$

These Lorentz scalar functions W_T and W_L are connected with the transverse or longitudinal photon absorption cross section σ_T and σ_L , respectively:

$$\begin{aligned} W_T &= 2\hat{p}_{\text{CM}} \sqrt{\hat{s}} \sigma_T(\gamma^* + b \rightarrow H + d), \\ W_L &= 2\hat{p}_{\text{CM}} \sqrt{\hat{s}} \sigma_L(\gamma^* + b \rightarrow H + d). \end{aligned} \quad (13)$$

Substituting Eqs. (12), (13) into (7), we finally obtain,

$$\begin{aligned} & \frac{d\sigma(\alpha + b \rightarrow \alpha + Q\bar{Q}_{[1,8]} + d)}{dQ^2 dy} \\ &= \frac{e_\alpha^2 \alpha_{\text{em}}}{4\pi Q^2} [2\rho^{++} \sigma_T(\gamma^* + b \rightarrow Q\bar{Q}_{[1,8]} + d) + \rho^{00} \\ & \quad \times \sigma_L(\gamma^* + b \rightarrow Q\bar{Q}_{[1,8]} + d)] f(s_{\alpha b}, p_{\text{CM}}, \hat{s}, \hat{p}_{\text{CM}}). \\ &= \frac{e_\alpha^2 \alpha_{\text{em}}}{2\pi} d\hat{t} F_b[n] \left[\frac{\rho^{++}}{Q^2} T_b[n] - \rho^{00} L_b[n] \right] f(s_{\alpha b}, p_{\text{CM}}, \hat{s}, \hat{p}_{\text{CM}}), \end{aligned} \quad (14)$$

where the relations: $d\sigma_T/d\hat{t} = F_b[n]T_b[n]$ and $d\sigma_L/d\hat{t} = -2Q^2 F_b[n]L_b[n]$, are employed. $F_b[n]$, $T_b[n]$ and $L_b[n]$ are the functions of Mandelstam variables \hat{s} , \hat{t} , \hat{u} , and Q^2 , which can be found in Ref. [27]. The coefficients

ρ^{ab} are the elements of the density matrix Eq. (5) in the γb -helicity basis:

$$\begin{aligned} 2\rho^{++} &= \epsilon_T^{\mu\nu} \rho_{\mu\nu} = \left[\frac{4(1-y)}{y^2} - \frac{4m_\alpha^2}{Q^2} \right] D(Q^2) + 2C(Q^2), \\ \rho^{00} &= \epsilon_L^{\mu\nu} \rho_{\mu\nu} = \frac{(2-y)^2}{y^2} D(Q^2) - C(Q^2). \end{aligned} \quad (15)$$

Here we come to the position to derive the second step of exact treatment, the detailed expressions of the form factors need to be discussed for each photon emission mechanism. In Martin-Ryskin method [51], the square of the electric proton form factor is employed as the coherent probability or weighting factor (WF) in p - p collisions: $w_{\text{coh}} = G_E^2(Q^2) = 1/(1+Q^2/0.71 \text{ GeV}^4)$, and the effect of the magnetic form factor is neglected. In the present paper, we extend this central idea to deal with the situation in heavy-ion collisions, where the magnetic form factor is also considered. In the case of coherent-photon emission, the photon emitter is nucleus, and the general notations $C(Q^2)$ and $D(Q^2)$ in Eq. (15) are the elastic nucleus form factors. In p - p collisions, α is proton, and $C(Q^2)$ and $D(Q^2)$ can be expressed as

$$\begin{aligned} D_{pp}^{\text{coh}}(Q^2) &= G_E^2(Q^2) \frac{4m_p^2 + 7.78Q^2}{4m_p^2 + Q^2}, \\ C_{pp}^{\text{coh}}(Q^2) &= 7.78G_E^2(Q^2). \end{aligned} \quad (16)$$

In Pb - Pb collisions, α is lead, $C(Q^2)$ and $D(Q^2)$ are

$$\begin{aligned} D_{PbPb}^{\text{coh}}(Q^2) &= Z^2 F_{\text{em}}^2(Q^2), \\ C_{PbPb}^{\text{coh}}(Q^2) &= \mu^2 F_{\text{em}}^2(Q^2), \end{aligned} \quad (17)$$

where

$$\begin{aligned} F_{\text{em}}(Q^2) &= \frac{3}{(QR_A)^3} [\sin(QR_A) \\ & \quad - QR_A \cos(QR_A)] \frac{1}{1 + a^2 Q^2}, \end{aligned} \quad (18)$$

is the electromagnetic form factor parameterization from the STARlight MC generator [52], in which $R_A = 1.1A^{1/3} \text{ fm}$, $a = 0.7 \text{ fm}$ and $Q = \sqrt{Q^2}$.

In the case of incoherent-photon emission, the remaining probability, $1 - w_{\text{coh}}$, has to be considered to avoid double counting. In p - p collisions, α is quarks inside the proton, and $C(Q^2)$ and $D(Q^2)$ can be written as

$$D_{pp}^{\text{incoh}}(Q^2) = C_{pp}^{\text{incoh}}(Q^2) = 1 - G_E^2(Q^2). \quad (19)$$

In Pb - Pb collisions, the incoherent-photon emission should further be distinguished as the ordinary-incoherent and ultra-incoherent photon emissions. For ordinary-incoherent photon emission, α is the protons inside the lead, and $D(Q^2)$ and $C(Q^2)$ are

$$\begin{aligned} D_{PbPb}^{\text{OIC}}(Q^2) &= [1 - F_{\text{em}}^2(Q^2)] D_{pp}^{\text{coh}}(Q^2), \\ C_{PbPb}^{\text{OIC}}(Q^2) &= [1 - F_{\text{em}}^2(Q^2)] C_{pp}^{\text{coh}}(Q^2), \end{aligned} \quad (20)$$

and for ultra-incoherent photon emission, α is the quarks inside the lead, since the neutron can not emit photon coherently, the WF for proton and neutron inside lead are different:

$$\begin{aligned} D_{PbPb}^{\text{UIC}}|_p(Q^2) &= C_{PbPb}^{\text{UIC}}|_p(Q^2) = [1 - F_{\text{em}}^2(Q^2)][1 - G_{\text{E}}^2(Q^2)], \\ D_{PbPb}^{\text{UIC}}|_n(Q^2) &= C_{PbPb}^{\text{UIC}}|_n(Q^2) = [1 - F_{\text{em}}^2(Q^2)]. \end{aligned} \quad (21)$$

B. The Q^2 and y distributions of heavy quarkonium production

Now we switch the general expression Eq. (14) to each specific channel in inelastic photoproduction processes. In the initial state, the inelastic photoproduction processes may be direct or resolved that are sensitive to the gluon distribution in the nucleus [4]. In the direct photoproduction process, the high-energy photon emitted from the projectile α , interacts with the partons of target nucleus B directly. In the resolved photoproduction process, the uncertainty principle allows the hadron-like photon for a short time to fluctuate into a state made of collinear quarks and gluons described by the virtual photon structure function, which then interacts with the partons of B by almost the purely strong interactions. Actually, as always with photons, the situation is quite complex. Together with the three different photon emission mechanisms mentioned in Section I, the complete description of the heavy quarkonium production requires the calculation of six classes of processes: coherent-direct (coh.dir.), coherent-resolved (coh.res.), ordinary-incoherent direct (OIC dir.), ordinary-incoherent resolved (OIC res.), ultra-incoherent direct (UIC dir.), and ultra-incoherent resolved (UIC res.) processes. These abbreviations will appear in many places of the remaining content.

In the case of coherent-direct process, the virtual photon emitted from the whole incident nucleus A interacts with parton b of target nucleus B , and A remains intact after photon emitted. The corresponding differential cross section can be derived as follows

$$\begin{aligned} & \frac{d\sigma_{\text{coh.dir.}}}{dQ^2 dy} (A + B \rightarrow A + H + X) \\ &= 2 \sum_b \int dx_b d\hat{t} f_{b/B}(x_b, \mu_b^2) \sum_n \langle \mathcal{O}_{[1,8]}^H[n] \rangle \\ & \times \frac{d\sigma}{dy dQ^2 d\hat{t}} (A + b \rightarrow A + Q\bar{Q}_{[1,8]}[n] + d), \end{aligned} \quad (22)$$

the factor of two arises because both nuclei emit photons and thus serve as targets.

In the case of ordinary-incoherent direct process, the virtual photon emitter is the proton a inside the nucleus A , the relevant differential cross section has the form of

$$\frac{d\sigma_{\text{OIC dir.}}}{dQ^2 dy} (A + B \rightarrow X_A + H + X)$$

$$\begin{aligned} &= 2Z_{Pb} \sum_b \int dx_b d\hat{t} f_{b/B}(x_b, \mu_b^2) \sum_n \langle \mathcal{O}_{[1,8]}^H[n] \rangle \\ & \times \frac{d\sigma}{dy dQ^2 d\hat{t}} (p + b \rightarrow p + Q\bar{Q}_{[1,8]}[n] + d), \end{aligned} \quad (23)$$

And in the case of ultra-incoherent direct processes, the virtual photon emitted from the quark a inside nucleus A interacts with parton b via the photon-quark Compton scattering and photon-gluon fusion, and A is allowed to break up after photon emitted. Similarly, the corresponding differential cross section is

$$\begin{aligned} & \frac{d\sigma_{\text{UIC dir.}}}{dQ^2 dy} (A + B \rightarrow X_A + H + X) \\ &= 2 \sum_{a,b} \int dx_a dx_b d\hat{t} f_{a/A}(x_a, \mu_a^2) f_{b/B}(x_b, \mu_b^2) \\ & \times \sum_n \langle \mathcal{O}_{[1,8]}^H[n] \rangle \frac{d\sigma}{dy dQ^2 d\hat{t}} (a + b \rightarrow a + Q\bar{Q}_{[1,8]}[n] + d), \end{aligned} \quad (24)$$

where the partonic cross section can be derived from Eq. (14) with $m_\alpha = m_q = 0$ and $e_\alpha = e_a$, where e_a is the charge of massless quark a .

In the coherent-resolved process, the parton a' of hadron-like photon which emitted from nucleus A , interacts with the parton b of target B via the interactions of quark-gluon Compton scattering, quark-antiquark annihilation and gluon-gluon fusion. The relevant differential cross section reads

$$\begin{aligned} & \frac{d\sigma_{\text{coh.res.}}}{dQ^2 dy} (A + B \rightarrow A + H + X) \\ &= 2 \sum_b \sum_{a'} \int dx_b dz_{a'} d\hat{t} f_{b/B}(x_b, \mu_b^2) f_{a'/\gamma}(z_{a'}, \mu_\gamma^2) \\ & \times \frac{Z_{Pb}^2 \alpha_{\text{em}}}{2\pi} \frac{y \rho_{\text{coh}}^{++}}{Q^2} \sum_n \langle \mathcal{O}_{[1,8]}^H[n] \rangle \frac{d\sigma_{a'b \rightarrow Q\bar{Q}_{[1,8]}[n]d}}{d\hat{t}}, \end{aligned} \quad (25)$$

where $z_{a'} = p_{a'}/q$ and $f_\gamma(z_{a'}, \mu_\gamma^2)$ denote the parton's momentum fraction and the parton distribution function of the resolved photon [53], respectively. The involved partonic cross sections can be found in Refs. [54].

In the ordinary-incoherent resolved process, the resolved photon emitter is the protons inside nucleus, and the relevant differential cross section is

$$\begin{aligned} & \frac{d\sigma_{\text{OIC res.}}}{dQ^2 dy} (A + B \rightarrow X_A + H + X) \\ &= 2Z_{Pb} \sum_b \sum_{a'} \int dx_b dz_{a'} d\hat{t} f_{b/B}(x_b, \mu_b^2) f_{a'/\gamma}(z_{a'}, \mu_\gamma^2) \\ & \times \frac{\alpha_{\text{em}}}{2\pi} \frac{y \rho_{\text{OIC}}^{++}}{Q^2} \sum_n \langle \mathcal{O}_{[1,8]}^H[n] \rangle \frac{d\sigma_{a'b \rightarrow Q\bar{Q}_{[1,8]}[n]d}}{d\hat{t}}. \end{aligned} \quad (26)$$

In the ultra-incoherent resolved process, the quark inside nucleus A emit a resolved virtual photon, then the parton

a' of this resolved photon interacts with parton b inside target B like a hadron, and A is break up after photon emitted. The relevant differential cross section is

$$\begin{aligned} & \frac{d\sigma_{\text{UIC}}^{\text{res.}}}{dQ^2 dy} (A + B \rightarrow X_A + H + X) \\ &= 2 \sum_{a,b} \sum_{a'} \int dx_a dx_b dz_{a'} d\hat{t} f_{a/A}(x_a, \mu_a^2) \\ & \quad \times f_{b/B}(x_b, \mu_b^2) f_{a'/\gamma}(z_{a'}, \mu_\gamma^2) \frac{e_a^2 \alpha_{\text{em}}}{2\pi} \frac{y \rho_{\text{UIC}}^{++}}{Q^2} \\ & \quad \times \sum_n \langle \mathcal{O}_{[1,8]}^H[n] \rangle \frac{d\sigma_{a'b \rightarrow Q\bar{Q}_{[1,8]}[n]d}}{d\hat{t}}. \end{aligned} \quad (27)$$

C. The p_T distribution of heavy quarkonium production

The distribution in p_T can be achieved using the Jacobian transformation. And in the final state, there are two types of inelastic heavy quarkonium photoproduction need to be distinguished: direct heavy quarkonium produced from the γ - g fusion, annihilation and Compton scattering of partons; fragmentation heavy quarkonium produced through the final fragmentation of a parton. We will take into account all of these aspects.

1. Direct heavy quarkonium production

For convenience, before doing the transformation the Mandelstam variables in γ^*b CM frame should be written as

$$\begin{aligned} \hat{s} &= (m_T \cosh y_r + \sqrt{\cosh^2 y_r m_T^2 + m_b^2 - M_H^2})^2 \\ \hat{t} &= M_H^2 - Q^2 - 2m_T (\hat{E}_\gamma \cosh y_r - \hat{p}_{\text{CM}} \sinh y_r), \\ \hat{u} &= M_H^2 + m_b^2 - 2m_T (\hat{E}_b \cosh y_r + \hat{p}_{\text{CM}} \sinh y_r), \end{aligned} \quad (28)$$

where y_r is the rapidity, $m_T = \sqrt{M_H^2 + p_T^2}$ is the transverse mass of heavy quarkonium, \hat{E}_γ , \hat{E}_b , and \hat{p}_{CM} are the energies and momentum in γ^*b CM frame, respectively. The details are presented in Appendix B.

In the case of direct photoproduction processes, the variables x_b and \hat{t} should be chosen to do the following transformation,

$$d\hat{t} dx_b = \mathcal{J} dy_r dp_T = \left| \frac{D(x_b, \hat{t})}{D(y_r, p_T)} \right| dy_r dp_T, \quad (29)$$

and then the relevant cross sections for direct heavy quarkonium production can be written as,

$$\begin{aligned} & \frac{d\sigma_{\text{coh.dir.}}}{dp_T} (A + B \rightarrow A + H + X) \\ &= 2 \sum_b \int dy_r dQ^2 dy f_{b/B}(x_b, \mu_b^2) \mathcal{J} \sum_n \langle \mathcal{O}_{[1,8]}^H[n] \rangle \\ & \quad \times \frac{d\sigma}{dQ^2 dy d\hat{t}} (A + b \rightarrow A + Q\bar{Q}_{[1,8]}[n] + d), \end{aligned} \quad (30)$$

$$\begin{aligned} & \frac{d\sigma_{\text{OIC}}^{\text{dir.}}}{dp_T} (A + B \rightarrow X_A + H + X) \\ &= 2Z_{Pb} \sum_b \int dy_r dQ^2 dy f_{b/B}(x_b, \mu_b^2) \mathcal{J} \sum_n \langle \mathcal{O}_{[1,8]}^H[n] \rangle \\ & \quad \times \frac{d\sigma}{dQ^2 dy d\hat{t}} (p + b \rightarrow p + Q\bar{Q}_{[1,8]}[n] + d), \end{aligned} \quad (31)$$

$$\begin{aligned} & \frac{d\sigma_{\text{UIC}}^{\text{dir.}}}{dp_T} (A + B \rightarrow X_A + H + X) \\ &= 2 \sum_{a,b} \int dy_r dQ^2 dy dx_a f_{a/A}(x_a, \mu_a^2) f_{b/B}(x_b, \mu_b^2) \mathcal{J} \\ & \quad \times \sum_n \langle \mathcal{O}_{[1,8]}^H[n] \rangle \frac{d\sigma}{dQ^2 dy d\hat{t}} (a + b \rightarrow a + Q\bar{Q}_{[1,8]}[n] + d). \end{aligned} \quad (32)$$

In the case of resolved contributions, we should choose the variables \hat{t}^* and $z_{a'}$ to do the similar transformation,

$$d\hat{t}^* dz_{a'} = \mathcal{J} dy_r dp_T = \left| \frac{D(z_{a'}, \hat{t}^*)}{D(y_r, p_T)} \right| dy_r dp_T, \quad (33)$$

the corresponding differential cross sections are

$$\begin{aligned} & \frac{d\sigma_{\text{coh.res.}}}{dp_T} (A + B \rightarrow A + H + X) \\ &= 2 \sum_b \sum_{a'} \int dy_r dQ^2 dy dx_b f_{b/B}(x_b, \mu_b^2) f_\gamma(z_{a'}, \mu_\gamma^2) \mathcal{J} \\ & \quad \times \frac{Z_{Pb}^2 \alpha_{\text{em}}}{2\pi} \frac{y \rho_{\text{coh}}^{++}}{Q^2} \sum_n \langle \mathcal{O}_{[1,8]}^H[n] \rangle \frac{d\sigma_{a'b \rightarrow Q\bar{Q}_{[1,8]}[n]d}}{d\hat{t}}, \end{aligned} \quad (34)$$

$$\begin{aligned} & \frac{d\sigma_{\text{OICres.}}}{dp_T} (A + B \rightarrow X_A + H + X) \\ &= 2Z_{Pb} \sum_b \sum_{a'} \int dy_r dQ^2 dy dx_b f_{b/B}(x_b, \mu_b^2) f_\gamma(z_{a'}, \mu_\gamma^2) \\ & \quad \times \mathcal{J} \frac{\alpha_{\text{em}}}{2\pi} \frac{y \rho_{\text{OIC}}^{++}}{Q^2} \sum_n \langle \mathcal{O}_{[1,8]}^H[n] \rangle \frac{d\sigma_{a'b \rightarrow Q\bar{Q}_{[1,8]}[n]d}}{d\hat{t}}, \end{aligned} \quad (35)$$

$$\begin{aligned} & \frac{d\sigma_{\text{UICres.}}}{dp_T} (A + B \rightarrow X_A + H + X) \\ &= 2 \sum_{a,b} \sum_{a'} \int dy_r dQ^2 dy dx_a dx_b f_{a/A}(x_a, \mu_a^2) \\ & \quad \times f_{b/B}(x_b, \mu_b^2) f_\gamma(z_{a'}, \mu_\gamma^2) \mathcal{J} e_a^2 \frac{\alpha_{\text{em}}}{2\pi} \frac{y \rho_{\text{UIC}}^{++}}{Q^2} \\ & \quad \times \sum_n \langle \mathcal{O}_{[1,8]}^H[n] \rangle \frac{d\sigma_{a'b \rightarrow Q\bar{Q}_{[1,8]}[n]d}}{d\hat{t}}, \end{aligned} \quad (36)$$

where the Mandelstam variables of resolved photoproduction are the same as Eq. (28), but with $Q^2 = 0$.

2. Fragmentation heavy quarkonium production

The fragmentation heavy quarkonium production is also an important channel which involves a nonperturbative part described by the heavy quarkonium fragmentation function, $D_{c \rightarrow Q\bar{Q}_{[1,8]}}(z_c, Q^2)$ [55, 56]. $z_c = 2p_T \cosh y_r / \sqrt{s}$ is the momentum fraction of the final state heavy quarkonium. Firstly, we should rewrite the Mandelstam variables as the following forms

$$\begin{aligned}\hat{s} &= y(s_{\alpha b} - m_\alpha^2 - m_b^2) - Q^2 + m_b^2, \\ \hat{t} &= \frac{1}{2 \cosh y_r} \left[Q^2(e^{y_r} - 2 \cosh y_r) - \frac{\hat{s}}{e^{y_r}} \right], \\ \hat{u} &= -(\hat{s} + Q^2) \frac{e^{y_r}}{2 \cosh y_r}.\end{aligned}\quad (37)$$

Then the variables z_c and \hat{t} can do the transformation

$$\hat{t} dz_c = \mathcal{J} dy_r dp_T = \left| \frac{D(z_c, \hat{t})}{D(y_r, p_T)} \right| dy_r dp_T. \quad (38)$$

For direct photoproduction processes, the relevant cross sections of fragmentation heavy quarkonium production are

$$\begin{aligned}& \frac{d\sigma_{\text{coh.dir.-frag.}}}{dp_T}(A + B \rightarrow p + H + X) \\ &= 2 \sum_{b,c} \int dy_r dQ^2 dy dx_b f_{b/B}(x_b, \mu_b^2) \mathcal{J} \sum_n \langle \mathcal{O}_{[1,8]}^H[n] \rangle \\ & \times \frac{D_{c \rightarrow Q\bar{Q}_{[1,8]}}(z_c, Q^2)}{z_c} \frac{d\sigma}{dQ^2 dy d\hat{t}}(A + b \rightarrow A + c + d),\end{aligned}\quad (39)$$

$$\begin{aligned}& \frac{d\sigma_{\text{OIC dir.-frag.}}}{dp_T}(A + B \rightarrow X_A + H + X) \\ &= 2Z_{Pb} \sum_{b,c} \int dy_r dQ^2 dy dx_b f_{b/B}(x_b, \mu_b^2) \mathcal{J} \sum_n \langle \mathcal{O}_{[1,8]}^H[n] \rangle \\ & \times \frac{D_{c \rightarrow Q\bar{Q}_{[1,8]}}(z_c, Q^2)}{z_c} \frac{d\sigma}{dQ^2 dy d\hat{t}}(p + b \rightarrow p + c + d),\end{aligned}\quad (40)$$

$$\begin{aligned}& \frac{d\sigma_{\text{UIC dir.-frag.}}}{dp_T}(A + B \rightarrow X_A + H + X) \\ &= 2 \sum_{a,b,c} \int dy_r dQ^2 dy dx_a dx_b f_{a/A}(x_a, \mu_a^2) \\ & \times f_{b/B}(x_b, \mu_b^2) \mathcal{J} \sum_n \langle \mathcal{O}_{[1,8]}^H[n] \rangle \frac{D_{c \rightarrow Q\bar{Q}_{[1,8]}}(z_c, Q^2)}{z_c} \\ & \times \frac{d\sigma}{dQ^2 dy d\hat{t}}(a + b \rightarrow a + c + d),\end{aligned}\quad (41)$$

where the involved partonic subprocesses are $q\gamma^* \rightarrow q\gamma$, $q\gamma^* \rightarrow qg$ and $g\gamma^* \rightarrow q\bar{q}$, the relevant cross sections were calculated in Ref. [5].

For resolved contributions, the differential cross sections are

$$\begin{aligned}& \frac{d\sigma_{\text{coh.res.-frag.}}}{dp_T}(A + B \rightarrow A + H + X) \\ &= 2 \sum_b \sum_{a',c} \int dy_r dQ^2 dy dx_b dz_{a'} f_{b/B}(x_b, \mu_b^2) \\ & \times f_\gamma(z_{a'}, \mu_\gamma^2) \mathcal{J} \frac{Z_{Pb}^2 \alpha_{\text{em}}}{2\pi} \frac{y \rho_{\text{coh}}^{++}}{Q^2} \frac{d\sigma_{a'b \rightarrow cd}}{d\hat{t}} \\ & \times \sum_n \langle \mathcal{O}_{[1,8]}^H[n] \rangle \frac{D_{c \rightarrow Q\bar{Q}_{[1,8]}}(z_c, Q^2)}{z_c},\end{aligned}\quad (42)$$

$$\begin{aligned}& \frac{d\sigma_{\text{OIC res.-frag.}}}{dp_T}(A + B \rightarrow X_A + H + X) \\ &= 2Z_{Pb} \sum_b \sum_{a',c} \int dy_r dQ^2 dy dx_b dz_{a'} \\ & \times f_{b/B}(x_b, \mu_b^2) f_\gamma(z_{a'}, \mu_\gamma^2) \mathcal{J} \frac{\alpha_{\text{em}}}{2\pi} \frac{y \rho_{\text{OIC}}^{++}}{Q^2} \\ & \times \frac{d\sigma_{a'b \rightarrow cd}}{d\hat{t}} \sum_n \langle \mathcal{O}_{[1,8]}^H[n] \rangle \frac{D_{c \rightarrow Q\bar{Q}_{[1,8]}}(z_c, Q^2)}{z_c},\end{aligned}\quad (43)$$

$$\begin{aligned}& \frac{d\sigma_{\text{UIC res.-frag.}}}{dp_T}(A + B \rightarrow X_A + H + X) \\ &= 2 \sum_{a,b} \sum_{a',c} \int dy_r dQ^2 dy dx_a dx_b dz_{a'} f_{a/A}(x_a, \mu_a^2) \\ & \times f_{b/B}(x_b, \mu_b^2) f_\gamma(z_{a'}, \mu_\gamma^2) \mathcal{J} \frac{e_a^2 \alpha_{\text{em}}}{2\pi} \frac{y \rho_{\text{UIC}}^{++}}{Q^2} \\ & \times \frac{d\sigma_{a'b \rightarrow cd}}{d\hat{t}} \sum_n \langle \mathcal{O}_{[1,8]}^H[n] \rangle \frac{D_{c \rightarrow Q\bar{Q}_{[1,8]}}(z_c, Q^2)}{z_c},\end{aligned}\quad (44)$$

where the involved subprocesses are $qq \rightarrow qq$, $qq' \rightarrow qq'$, $q\bar{q} \rightarrow q\bar{q}$, $q\bar{q} \rightarrow q'\bar{q}'$, $q\bar{q}' \rightarrow q\bar{q}'$, $qg \rightarrow q\gamma$, $qg \rightarrow qg$ and $gg \rightarrow q\bar{q}$ [57]. The Mandelstam variables of resolved contributions are the same as Eq. (37), but with $Q^2 = 0$.

III. WEIZSÄCKER-WILLIAMS APPROXIMATION

The connection between the process in Fig. 1(a) and (b) is evident. By treating the moving electromagnetic fields of charged particle as a flux of quasi-real photons, the photoproduction process can be expressed in terms of the real photo-absorption cross section with the photon spectrum. This idea belongs to Fermi [12], and was used and developed for the calculation of the cross section of interaction of relativistic charged particles by Weizsäcker and Williams, and the method is now known as the Weizsäcker-Williams approximation (WWA) [13]. An essential advantage of WWA consists in the fact that, when using it, it is sufficient to obtain the photo-absorption

cross section on the mass shell only. Details of its off mass-shell behavior are not essential. In the present section, we switch the accurate expression Eq. (14) into the WWA form and discuss a number of widely employed photon spectra. The exact treatment developed in Section II can reduce to the WWA near the region $Q^2 \sim 0$. When switching to the approximate formulae of WWA, two simplifications should be performed. First, the scalar photon contribution σ_L is neglected; secondly, the term of σ_T is substituted by its on-shell value. This provides us a powerful approach to study the properties of WWA.

Taking $Q^2 \rightarrow 0$, Eq. (14) turns into:

$$\begin{aligned} & \lim_{Q^2 \rightarrow 0} d\sigma(\alpha + b \rightarrow \alpha + Q\bar{Q}_{[1,8]} + d) \\ &= \left[\frac{e_\alpha^2 \alpha_{\text{em}}}{2\pi} (y\rho^{++}) \frac{dy dQ^2}{Q^2} \right] \sigma_T \frac{\hat{p}_{\text{CM}} \sqrt{\hat{s}}}{yp_{\text{CM}} \sqrt{s_0}} \Big|_{Q^2=0} \\ &= \sigma_T dn_\gamma \Big|_{Q^2=0}, \end{aligned} \quad (45)$$

where the contribution of σ_L and the terms proportional to Q^2 are neglected in the limit $Q^2 \rightarrow 0$. And the general form of the photon spectrum $f_\gamma(y)$, which is associated with various particles, reads

$$\begin{aligned} f_\gamma(y) &= \frac{dn_\gamma}{dy} = y \int \frac{dQ^2}{Q^2} \frac{e_\alpha^2 \alpha_{\text{em}}}{2\pi} \rho^{++} \\ &= \frac{e_\alpha^2 \alpha_{\text{em}}}{2\pi} \int \frac{dQ^2}{Q^2} \left\{ yC(Q^2) + \left[\frac{2(1-y)}{y} - \frac{2ym_\alpha^2}{Q^2} \right] D(Q^2) \right\}. \end{aligned} \quad (46)$$

In the case of coherent-photon emission, Ref. [6] presented a modified photon flux function of proton from Eq. (46). By neglecting the effects of the magnetic form factor and adopting the dipole form of electric form factor of proton: $C(Q^2) = D(Q^2) = G_E^2(Q^2)$, and employing the coherent condition $Q^2 \leq 1/R_A^2$ ($Q_{\text{max}}^2 = 0.027, y_{\text{max}} = 0.16$), one obtains with $a = 2m_p^2/Q_{\text{max}}^2$ and $b = 2m_p^2/0.71 = 2.48$,

$$\begin{aligned} f^{\text{MD}}(y) &= \frac{\alpha_{\text{em}}}{2\pi} y [a - 2x + (2x + c_1)d_1 + (2x + c_2)d_2 \\ &\quad + (3x + c_3)d_3 + (2x + c_4)d_4], \end{aligned} \quad (47)$$

where x depends on y ,

$$x = -\frac{1}{y} + \frac{1}{y^2}. \quad (48)$$

Actually, the origin of various practically employed photon spectra is another plane wave form, which is given in Ref. [50] and can be written as follows

$$\begin{aligned} & dn_\gamma(y) \\ &= \frac{e_\alpha^2 \alpha_{\text{em}}}{\pi} \frac{dy}{y} \frac{dQ^2}{Q^2} \left[\frac{y^2}{2} D(Q^2) + (1-y) \frac{Q^2 - Q_{\text{min}}^2}{Q^2} C(Q^2) \right], \end{aligned} \quad (49)$$

this form is achieved from the complete expression Eq. (46) by assuming that, $Q_{\text{min}}^2 = y^2 m_\alpha^2 / (1-y)$, which is the LO term of the following complete expression in the expansion of $\mathcal{O}(m_\alpha^2)$,

$$\begin{aligned} Q_{\text{min}}^2 &= -2m_\alpha^2 + \frac{1}{2s_{ab}} [(s_{ab} + m_\alpha^2)(s_{ab} - \hat{s} + m_\alpha^2) \\ &\quad - (s_{ab} - m_\alpha^2) \sqrt{(s_{ab} - \hat{s} + m_\alpha^2)^2 - 4s_{ab}m_\alpha^2}]. \end{aligned} \quad (50)$$

This approximation is only available when $m_\alpha^2 \ll 1 \text{ GeV}^2$, however m_p^2 and m_{Pb}^2 do not satisfy this condition; this is a source of error in various spectra. Especially for lead, this approximation will lead erroneous results.

Drees and Zeppenfeld (DZ) provided another widely used photon distribution function of proton [15–21], which is the approximate analytic form of Eq. (49). Based on the assumptions: $Q_{\text{max}}^2 \rightarrow \infty$, $C(Q^2) = D(Q^2) = G_E^2(Q^2)$, and $Q^2 - Q_{\text{min}}^2 \approx Q^2$, they obtained

$$\begin{aligned} & f^{\text{DZ}}(y) \\ &= \frac{\alpha_{\text{em}}}{2\pi} \frac{1 + (1-y)^2}{y} \left(\ln A - \frac{11}{6} + \frac{3}{A} - \frac{3}{2A^2} + \frac{1}{3A^2} \right), \end{aligned} \quad (51)$$

where $A = (1 + 0.71 \text{ GeV}/Q_{\text{min}}^2)$. In Ref. [28], Drees, Ellis, and Zeppenfeld (DEZ) also performed a spectrum of lead. Based on the assumptions $y \ll 1$, $Q_{\text{max}}^2 \sim \infty$, $C_{Pb}(Q^2) = 0$, and $D_{Pb}(Q^2) \approx \exp(-\frac{Q^2}{Q_0^2})$, they achieved,

$$\begin{aligned} & f^{\text{DEZ}}(y) \\ &= \frac{\alpha_{\text{em}}}{\pi} \left[-\frac{\exp(-Q_{\text{min}}^2/Q_0^2)}{y} + \left(\frac{1}{y} + \frac{M^2}{Q_0^2} y \right) \Gamma(0, \frac{Q_{\text{min}}^2}{Q_0^2}) \right], \end{aligned} \quad (52)$$

where $Q_{\text{min}}^2 = m_{Pb}^2 y^2$, $\Gamma(a, Q_{\text{min}}^2/Q_0^2) = \int_y^\infty t^{a-1} e^{-t} dt$. It should be noticed that, $y \ll 1$ means $Q_{\text{max}}^2 \ll 1$, which contradicts with the assumption $Q_{\text{max}}^2 \sim \infty$.

Based on Eq. (51), Nystrand derived a modified photon spectrum of proton which include the Q_{min}^2 term in Eq. (49) and can be presented as [25]

$$\begin{aligned} & f^{\text{Ny}}(y) \\ &= \frac{\alpha_{\text{em}}}{2\pi} \frac{1 + (1-y)^2}{y} \left[\frac{A+3}{A-1} \ln A - \frac{17}{6} - \frac{4}{3A} + \frac{1}{6A^2} \right]. \end{aligned} \quad (53)$$

In addition, the effect of including the magnetic form factor of the proton has been estimated by Kniehl [22]. The final expression $f^{\text{Kn}}(y)$ (Eq. (3.11) of Ref. [22]) is too long to include here, but will be discussed further below.

Another most important approach for coherent photon spectrum is the semiclassical impact parameter description, which excludes the hadronic interaction easily. The

relevant calculation is explained in Ref. [58], and the result can be written as

$$f^{\text{SC}}(y) = \frac{2Z^2\alpha_{\text{em}}}{\pi} \left(\frac{c}{v}\right)^2 \frac{1}{y} \left[\xi K_0 K_1 + \frac{\xi^2}{2} \left(\frac{v}{c}\right)^2 (K_0^2 - K_1^2) \right], \quad (54)$$

where v is the velocity of the point charge Ze , $K_0(x)$ and $K_1(x)$ are the modified Bessel functions, and $\xi = b_{\text{min}} m_A y / v$.

In the case of incoherent-photon emission, the actually used photon spectrum can be derived from Eq. (49), by neglecting the weighting factor in Eqs. (19) and (21), and setting $Q_{\text{min}}^2 = 1 \text{ GeV}^2$ and $Q_{\text{max}}^2 = \hat{s}/4$ [59],

$$f^{\text{incoh}}(y) = e_\alpha^2 \frac{\alpha_{\text{em}}}{2\pi} \frac{1 + (1-y)^2}{y} \ln \frac{Q_{\text{max}}^2}{Q_{\text{min}}^2}. \quad (55)$$

Finally, another important form of incoherent photon spectrum was calculated by Brodsky, Kinoshita and Terazawa in Ref. [60], which is originally derived for ep scattering and can be expressed as

$$f^{\text{BKT}}(y) = \frac{e_\alpha^2 \alpha_{\text{em}}}{\pi} \left\{ \frac{1 + (1-y)^2}{y} \left(\ln \frac{E}{m} - \frac{1}{2} \right) + \frac{y}{2} \left[\ln \left(\frac{2}{y} - 2 \right) + 1 \right] + \frac{(2-y)^2}{2y} \ln \left(\frac{2-2y}{2-y} \right) \right\}. \quad (56)$$

IV. NUMERICAL RESULTS

We are now in a position to provide our numerical results. The mass of proton is $m_p = 0.938 \text{ GeV}$ [61]. The strong coupling constant is taken as the one-loop form [62]

$$\alpha_s = \frac{12\pi}{(33 - 2n_f) \ln(\mu^2/\Lambda^2)}, \quad (57)$$

with $n_f = 3$ and $\Lambda = 0.2 \text{ GeV}$. The wavefunctions and the MEs of heavy quarkonium, and the full kinematical relations are summarized in Appendices. In addition, the coherence condition ($Q^2 \leq 1/R_A^2$) [2] is adopted in coherent-photon emission, which limits Q^2 and y to very low values, $Q_{\text{max}}^2 = 0.027 \text{ GeV}^2$ and $7.691 \times 10^{-4} \text{ GeV}^2$, and $y_{\text{max}} \sim 0.16$ and 1.42×10^{-4} , for proton and lead, respectively. Finally, the differential cross section for the LO initial partons hard scattering (had.sc. and had.sc.-frag.) are

$$d\sigma_{\text{had.sc.}} = \sum_{a,b} \int dx_a dx_b f_{a/A}(x_a, \mu_a^2) f_{b/B}(x_b, \mu_b^2) \times \sum_n \langle \mathcal{O}^H[n] \rangle d\sigma_{ab \rightarrow Q\bar{Q}_{[1,8]}[n]d}, \quad (58)$$

$$d\sigma_{\text{had.sc.}-\text{frag.}} = \sum_{a,b,c} \int dx_a dx_b dz_c f_{a/A}(x_a, \mu_a^2) f_{b/B}(x_b, \mu_b^2) \times \sum_n \langle \mathcal{O}^H[n] \rangle \frac{D_{c \rightarrow Q\bar{Q}_{[1,8]}[n]}(z_c, Q^2)}{z_c} d\sigma_{ab \rightarrow cd}, \quad (59)$$

the partonic cross sections were calculated in Ref. [57].

First of all, we choose the J/ψ as an example, to comprehensively study the features of WWA in heavy quarkonium production in ultrarelativistic heavy-ion collisions. In Fig. 2, the left panel shows the relative errors with respect to the exact results. The central and right panels show the exact results of Q^2 dependent differential cross sections in p - p and Pb - Pb collisions, respectively. In left panel, the relative errors can be neglected in small Q^2 region, but become evident when $Q^2 > 1 \text{ GeV}^2$. The relative error in Pb - Pb collisions is comparable with the one in p - p collisions around $Q^2 \sim 10 \text{ GeV}^2$, and becomes much larger when $Q^2 > 10^2 \text{ GeV}^2$. Therefore, WWA is only suitable in very small Q^2 domain, its error become evident when $Q^2 > 1 \text{ GeV}^2$. WWA has the higher accuracy in Pb - Pb collisions, however its error in large Q^2 region also become much larger in this case.

In central and right panels, we find that the contributions of coherent and ultra-incoherent photon emissions dominate the small and large Q^2 regions, respectively. They become comparable around $Q^2 = 0.1 \text{ GeV}^2$. We also observe that the contribution of ordinary-incoherent photon emission is important at the region $0.1 < Q^2 < 10 \text{ GeV}^2$. Comparing with the views derived from left panels, one can see that WWA can be a good approximation for coherent and ordinary incoherent-photon emissions, and is not a effective approximation for ultra-incoherent photon emission.

In Fig. 3, the results are expressed as a function of y . In panel (a), the WWA results nicely agree with the exact ones when $y < 0.5$ in the case of coherent photon emission, the difference appears with increasing y , especially when $y > 0.7$ the difference becomes evident. Inversely, the relative error are prominent in the whole y regions in the case of ultra-incoherent photon emission. In panels (b) and (c), the coherent- and ordinary-incoherent photon emissions are important in small y domain, and rapidly deceased with y increasing. On the contrary, the contribution of ultra-incoherent photon emission is important in the whole y regions and much higher than those of coherent ones. Therefore, WWA can be a good approximation for heavy quarkonium production when $y < 0.5$, although its error is evident at large values of y . One exception is the case of ultra-incoherent processes, where the WWA is inapplicable in the whole y regions.

In Fig. 4, the total cross sections are expressed as a function of \sqrt{s} . In left panel, the curves show a pronounced rising when $\sqrt{s} < 400$ and 200 GeV in p - p and Pb - Pb collisions, respectively. And they slowly decreased with increasing \sqrt{s} . Therefore, WWA has the significant

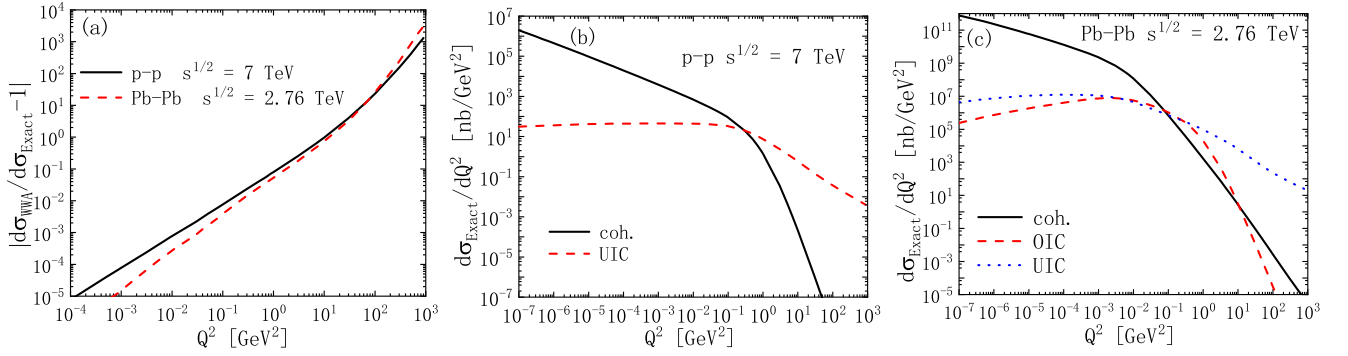


FIG. 2: The Q^2 distribution of J/ψ photoproduction at LHC energies. The left panel shows the relative errors with respect to the exact results for p - p and Pb - Pb collisions, respectively. The central and right panels show the exact results of Q^2 dependent differential cross sections in p - p and Pb - Pb collisions, respectively. (b), (c): Black solid line—coherent-photon emission [coh.(dir.+res.)]. Red dash line—incoherent-photon emission [incoh.(dir.+res.)] in panel (b) and ordinary-incoherent photon emission [OIC (dir.+res.)] in panel (c). Blue dot line—ultra-incoherent photon emission [UIC (dir.+res.)].

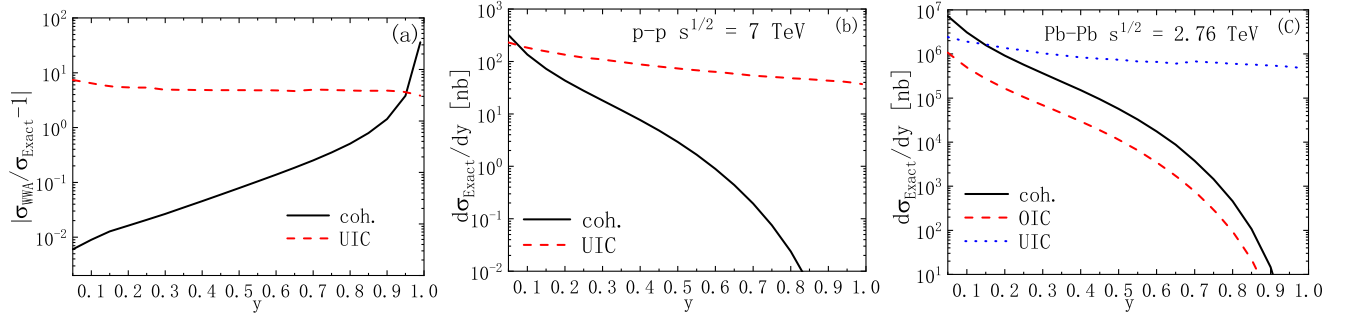


FIG. 3: Same as Fig. 2 but for y distribution. (a): the relative errors of OIC are the same as coh. one.

errors in small \sqrt{s} domains (RHIC energies), and have a good accuracy at high energies (LHC energies).

In central and right panels, the contribution of coherent-photon emission is slightly smaller than the ultra-incoherent one in p - p collisions; while the situation is opposite in Pb - Pb collisions, where the coherent-photon emission starts to play the very important role in the production processes (it is about one and two orders of magnitudes (OOMs) larger than ordinary- and ultra-incoherent photon emissions, respectively). The reason is that the coherent photon emission is proportional to Z^2 , whereas the ordinary- and ultra-incoherent photon emissions are only proportional to Z and N_A , respectively. As for $Z \gg 1$ the coherent part is dominant in the photoproduction. Together with the views derived in the left panel, we can deduce that WWA can reach the high accuracy in Pb - Pb collisions at LHC energies, where the incoherent contribution is suppressed; however it is not a good approximation in p - p collisions, where the incoherent contribution is comparable with the coherent one.

In Tables I-IV, the total cross sections are calculated to discuss the accuracies and the features of the widely employed photon spectra which are mentioned in Section III. In the case of coherent-photon emission [Table I, II], the relative errors are generally evident. The common reason is that the integrations of these spectra are performed in

TABLE I: Total cross sections of the heavy quarkonium photoproduction in the channel of coherent-photon emission in p - p collisions.

Coherent $\sqrt{s} = 7$ TeV	coh.dir.		coh.res.	
	σ [nb]	δ^a [%]	σ [nb]	δ [%]
Exact	48.5774	0.00	11.4139	0.00
f_{DZ}	93.1149	91.68	28.1579	146.70
f_{Ny}	75.3936	55.20	21.3935	87.43
f_{Kn}	85.6922	76.40	25.8231	126.24
f_{SC}	57.0919	17.53	14.6512	28.36
f_{MD}	48.8202	0.50	11.5982	1.61

^a Relative error with respect to the exact result: $\delta = |\sigma/\sigma_{\text{Exact}} - 1|$.

TABLE II: Same as Table I but in Pb - Pb collisions.

Coherent $\sqrt{s} = 2.76$ TeV	coh.dir.		coh.res.	
	σ [mb]	δ [%]	σ [mb]	δ [%]
Exact	5.0791	0.00	0.5563	0.00
f_{DEZ}	37.8744	645.68	7.2798	1208.69
f_{SC}	1.5664	69.16	0.2511	54.86

the entire kinematical allowed regions: $Q_{\text{max}}^2 = \infty$ and $y_{\text{max}} = 1$ which include the large WWA errors. In p - p collisions [Table I], the relative errors of f^{DZ} are the largest,

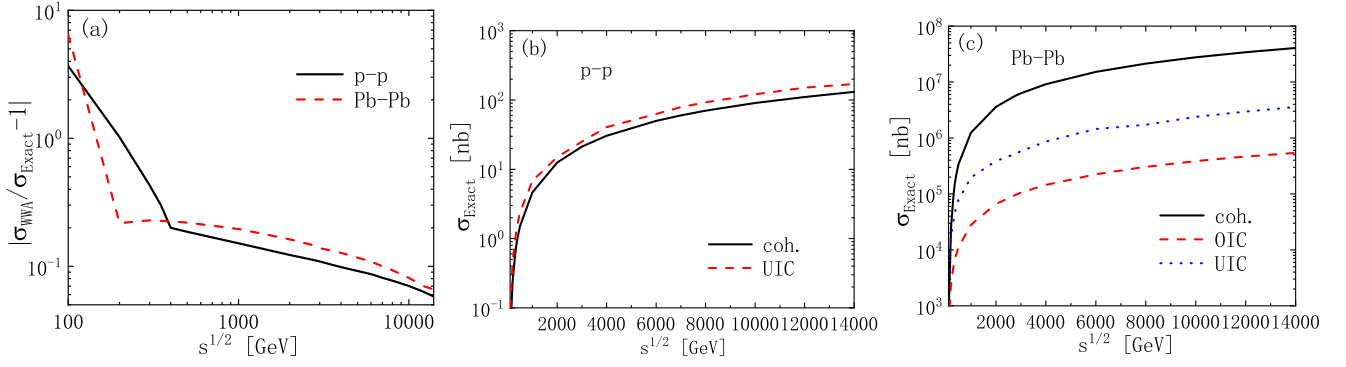


FIG. 4: Same as Fig. 2 but for the total cross sections as a function of \sqrt{s} .

TABLE III: Same as Table I but in the channel of ordinary-incoherent photon emission in $Pb-Pb$ collisions.

OIC $\sqrt{s} = 2.76$ TeV	OIC dir.		OIC res.	
	σ [mb]	δ [%]	σ [mb]	δ [%]
Exact	0.0779	0.00	0.0180	0.00
f_{DZ}	0.3462	344.40	0.0835	365.16
f_{Ny}	0.2787	257.76	0.0624	247.86
f_{Kn}	0.3185	308.84	0.0765	326.04
f_{SC}	0.1443	85.28	0.0248	38.04
f_{MD}	0.1780	128.49	0.0323	79.66

TABLE IV: Same as Table I but for ultra-incoherent photon emission in $p-p$ [7 TeV] and $Pb-Pb$ [2.76 TeV] collisions.

UIC	UIC dir.			UIC res.		
	Exact	$f_{\gamma/q}$	f_{BKT}	Exact	$f_{\gamma/q}$	f_{BKT}
σ_{pp} [μb]	0.02	0.20	0.32	0.05	0.06	0.09
δ_{pp} [%]	0.0	828.9	1397.9	0.0	25.8	103.8
σ_{PbPb} [mb]	0.20	1.17	2.84	0.32	0.28	0.68
δ_{PbPb} [%]	0.0	499.8	1355.1	0.0	13.3	110.4

but it still has one advantage that the electric form factor of proton is included in this form, which properly describes the situation of the proton as photon emitter. Since the WWA is usually adopted in electroproduction processes, if one directly obtains the spectrum of proton from that of electron by just replacing the m_e with m_p , it would extensively overestimate the cross section. The relative errors of f_{Ny} have a obvious reduction compared to those of f_{DZ} , since f_{Ny} includes the Q_{min}^2 term in Eq. (49) which is omitted in f_{DZ} , thus this term has the noticeable contribution and can not be neglected when performing the photon spectra; this agree with the perspectives of Kniehl in Ref. [22]. The relative errors of f_{Kn} are higher than those of f_{Ny} , since the effect of magnetic form factor of proton is included, which actually should be excluded in the coherent case [5]. In $Pb-Pb$ collisions [Table II], the relative errors of f_{DEZ} reach up to 1200%, since f_{DEZ} is based on the contradictory assumptions: $Q_{max}^2 \sim \infty$ and $y \ll 1$ ($Q_{max}^2 \sim \infty$ means $y_{max} = 1$).

In addition, the errors of f_{SC} in $p-p$ collisions are smallest, but it cause the too small results compared to the exact ones in $Pb-Pb$ collisions. One should cautious that when using f_{SC} in the calculation, $y_{max} = 1$ will cause the erroneous results, the coherence condition should be adopted. Finally, the modified proton spectra f_{MD} nicely agree with the exact ones. Since this form has two virtues: except considering kinematical boundaries, f_{MD} also adopts the coherence condition which effectively cut the WWA errors; it is derived from the complete form Eq. (46) which properly includes the Q_{min}^2 term and excludes the effects of magnetic form factor.

Table III is similar to Table I but for ordinary-incoherent photon emission, where the relative errors are much more evident. Even the modified photon spectrum f_{MD} can not give the accurate results. The reason is that the weighting factor “ $1 - F_{em}^2$ ” is neglected in these spectra in this case; this will cause the serious double counting, and we will see that this problem is much more serious in Table IV. In the case of ultra-incoherent photon emission [Table IV], we observe that the relative errors of the WWA parameterizations are prominent and become much larger in $Pb-Pb$ collisions. This quantitatively verifies the inapplicability of WWA in ultra-incoherent processes. For $f_{\gamma/q}$, its errors should be much higher than the values given in Table IV, since the weighting factor “ $(1 - F_{em}^2)(1 - G_E^2)$ ” is omitted. However, an artificial cutoff $Q_{min}^2 = 1 \text{ GeV}^2$ is used to cut the divergence from the small Q^2 region, but we can see that the results are still not accurate. For f_{BKT} , its errors are the largest, since f_{BKT} is originally derived from ep scattering, but is directly expanded to describe the probability of finding a photon in any relativistic fermion and to deal with hadronic collisions in Refs. [20–22], this will overestimate the cross sections. Therefore, the accurate expression Eq. (14) should be employed for the ultra-incoherent photon emission. And the results in Refs. [15–31] are not accurate enough, where the mentioned spectra are adopted and the serious double counting exists.

Here we adopt the exact treatment to present the p_T -dependent cross sections for heavy quarkonium productions. In Figs. 5-6, we plot the contribution of the charmonium (J/ψ , $\psi(2S)$, η_c , h_c and χ_{cJ}) photoproduction

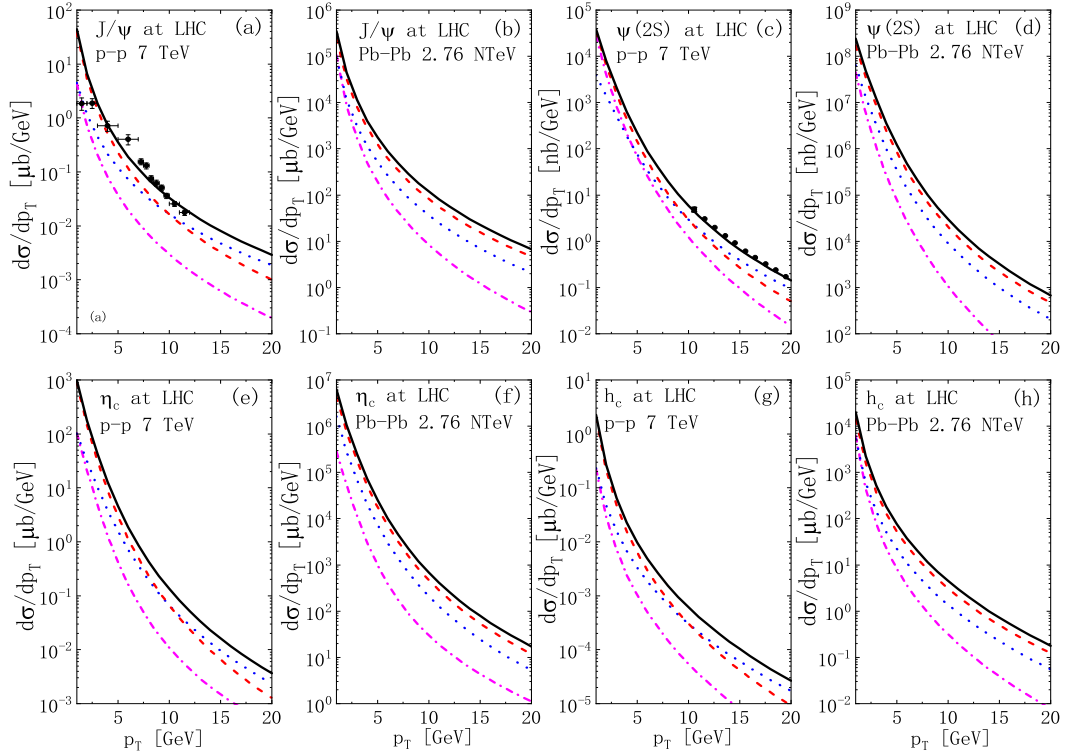


FIG. 5: The p_T distribution of J/ψ , $\psi(2S)$, η_c , and h_c photoproductions at LHC energies. Magenta dash dot and blue dot lines are for direct and fragmentation charmonium photoproductions, respectively. Red dash lines denote the initial partons hard scattering (had.sc.). Black solid lines are for the sum of the above processes. The J/ψ and $\psi(2S)$ data are from Refs. [63].

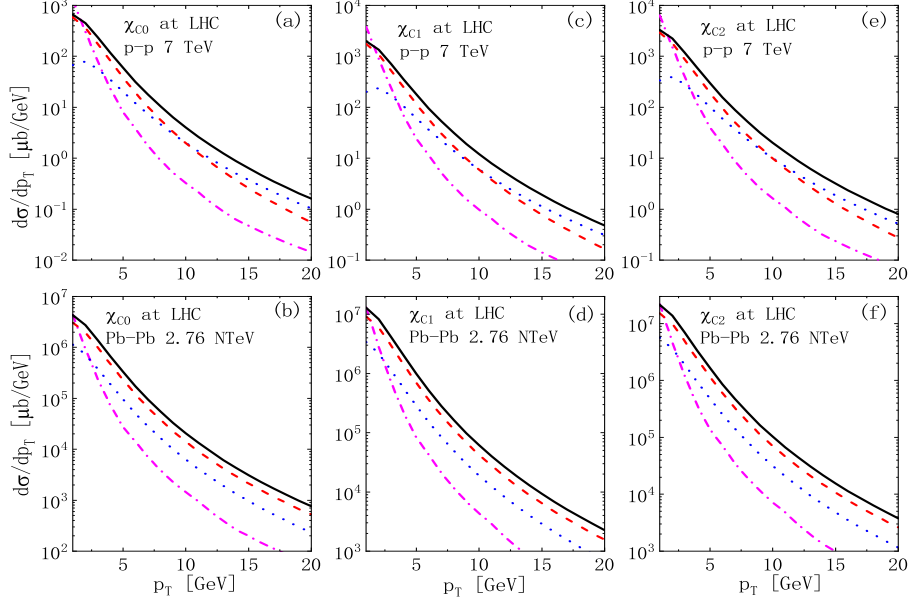


FIG. 6: Same as Fig 5, but for χ_{cJ} productions.

and fragmentation processes for p - p and Pb - Pb collisions at LHC energies, where all the results are the sum of direct and resolved contributions. The charmonium spectra of photoproduction and fragmentation processes are compared to the LO hard scattering of initial partons (had.sc.). In panels Fig. 5 (a) and (c), we compare

the exact results with data derived from relevant collaborations. Since the intrinsic motion of incident partons inside colliding hadrons renders the differential cross section uncertain for $p_T < 2$ GeV, we have not attempt to remove the divergences from the small p_T domain. Instead, we simply regard the portion of the plot which

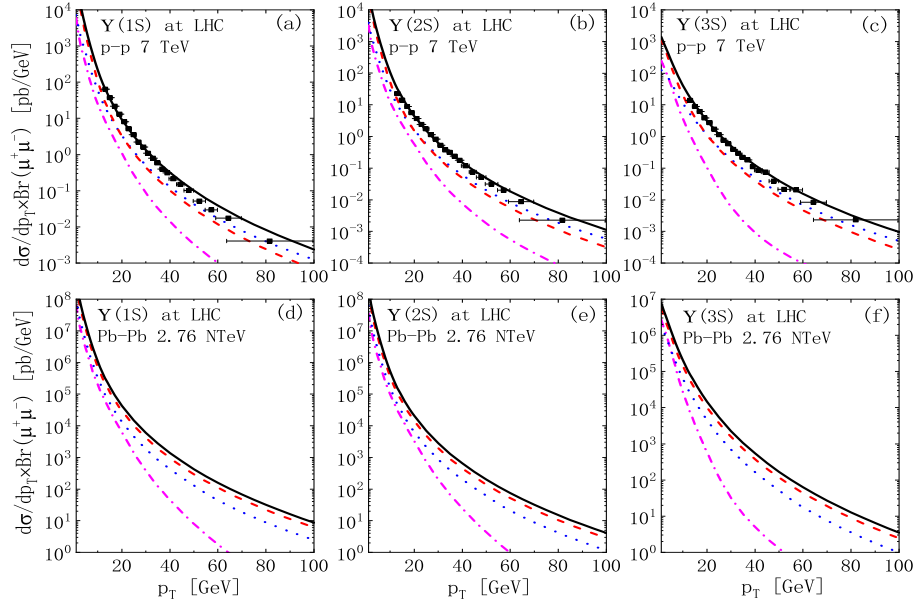


FIG. 7: Same as Fig 5, but for $\Upsilon(nS)$ productions. The branching fractions are $Br(\Upsilon(1S) \rightarrow \mu^+\mu^-) = 2.48\%$, $Br(\Upsilon(2S) \rightarrow \mu^+\mu^-) = 1.93\%$, and $Br(\Upsilon(3S) \rightarrow \mu^+\mu^-) = 2.18\%$. The $\Upsilon(nS)$ data are from Ref. [64].

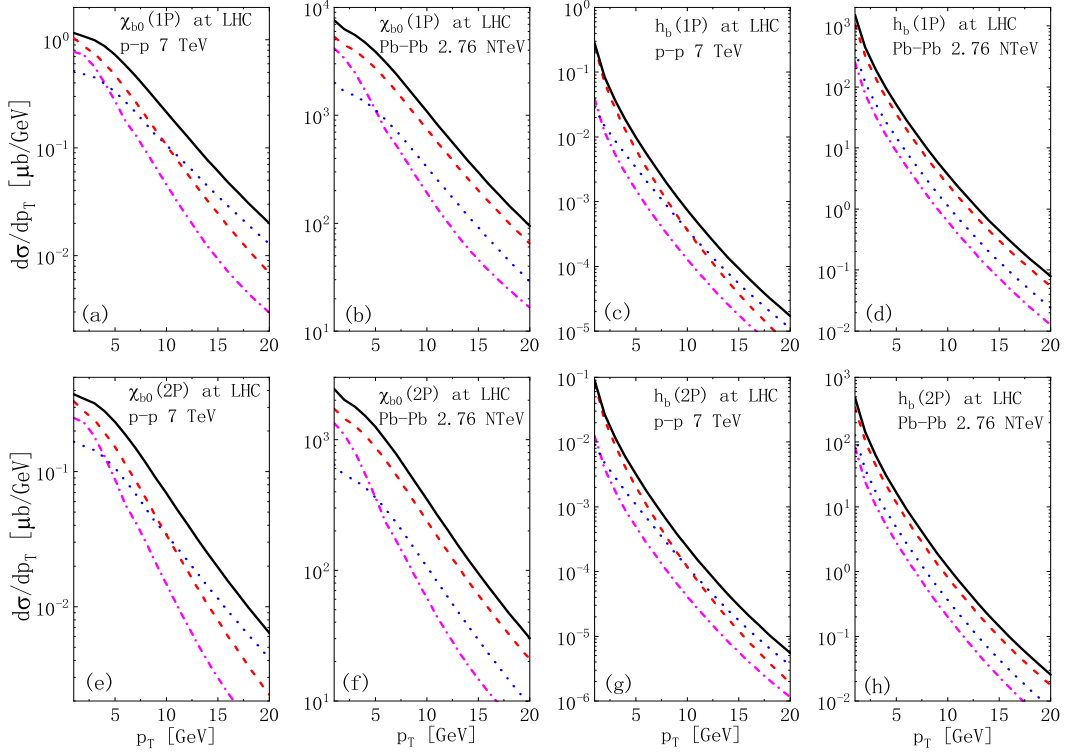


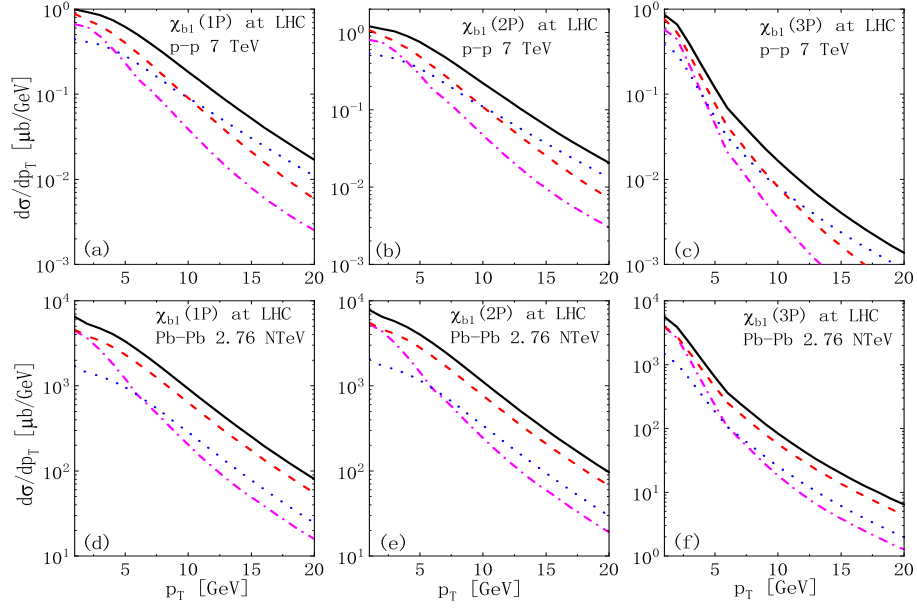
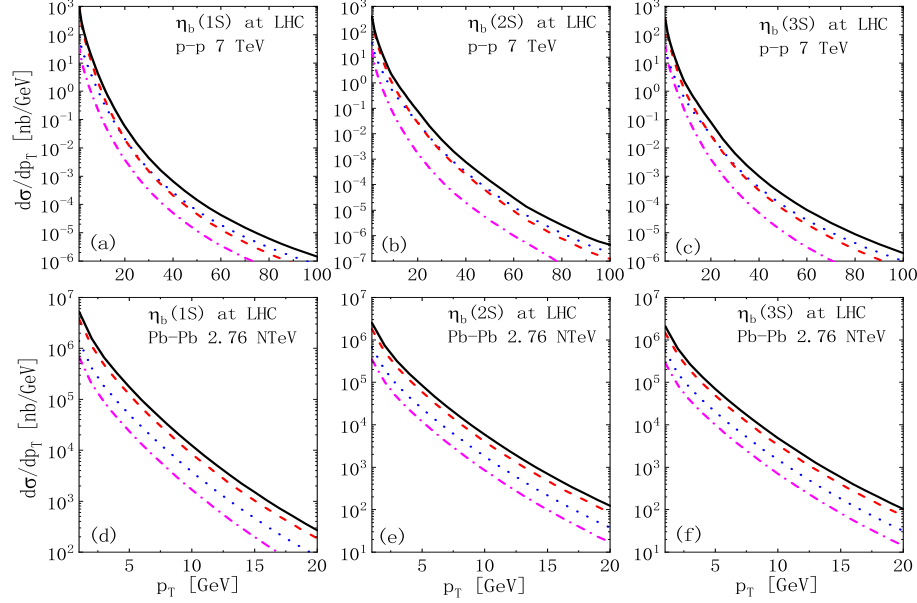
FIG. 8: Same as Fig 5, but for χ_{b0} and h_b productions.

runs below $p_T = 2$ GeV as untrustworthy.

We find that the charmonium photoproduction processes give the prominent corrections to LO had.sc. in the region of $p_T > 3$ GeV for p - p collisions at $\sqrt{s} = 7$ TeV, and of almost the whole p_T range for Pb - Pb collisions at $\sqrt{s} = 2.76$ TeV. Indeed, we also observe that the fragmentation charmonium photoproduction are gener-

ally about an OOM larger than direct charmonium photoproduction in the large p_T domain; it is even larger than the LO had.sc. when $p_T > 10$ GeV in p - p collisions. Thus, fragmentation processes are the main channel of photoproduction processes.

In Figs. 7-10, we also plot the exact results of bottomonium ($\Upsilon(nS)$, χ_{bJ} , h_b , and η_b) photoproduction and

FIG. 9: Same as Fig 5, but for χ_{b1} productions.FIG. 10: Same as Fig 5, but for η_b productions.

fragmentation processes for p - p and Pb - Pb collisions at LHC energies. In upper panels of Fig. 7, we compare the exact results with data derived from relevant collaborations for p - p collisions with $\sqrt{s} = 7$ TeV. We find that the contributions of photoproduction and fragmentation processes are still evident in bottomonium production.

V. SUMMARY AND CONCLUSIONS

In the framework of the NRQCD, we have investigated the production of heavy quarkonium by inelastic photoproduction and fragmentation processes in heavy-ion

collisions at LHC energies. The exact treatment is derived by performing a consistent analysis of the terms neglected in going from the accurate expression to the WWA one, which can effectively suppress the WWA errors and naturally weight the contributions from different charged sources. And the full partonic kinematics matched with exact treatment is also obtained. We presented a comprehensive study for the properties of WWA in heavy quarkonium photoproduction in heavy-ion collisions at LHC energies, by discussing the Q^2 -, y -, and \sqrt{s} -dependence behaviours of WWA. The total cross sections were also calculated to estimate the errors exist in the widely employed photon spectra. In the sequel, we

calculated the p_T -dependent cross sections to discuss the relative contributions of photoproduction and fragmentation processes to LO ones.

The numerical results indicate that the contribution of ultra-incoherent photon emission can not be neglected in the inelastic heavy quarkonium production, it provides the meaningful contributions; it is even larger than the coherent one in p - p collisions. In addition, the contributions of photoproduction and fragmentation processes are evident in the heavy quarkonium production, especially in the large p_T regions; while the fragmentation processes plays a important role, it is even larger than the LO one when $p_T > 10$ GeV in p - p collisions.

Furthermore, the WWA is only effective in very restricted domains, and its error is significance in small \sqrt{s} . The mentioned equivalent photon spectra generally have the obvious errors. And the double counting exists when the different channels are considered simultaneously, this trouble is much more serious in Pb - Pb collisions. WWA can only be used in the channel of coherent and ordinary-incoherent photon emissions, and is inapplicable in ultra-incoherent photon emission. These features permit one to employ the WWA as a roughly approximation (the error is about 10%) in Pb - Pb collisions, since the coherent contribution is enhanced by Z_{Pb}^2 . However WWA can not be used in p - p collisions, where the incoherent contribution becomes dominant. Indeed, the exact treatment is needed to deal accurately with the inelastic heavy quarkonium photoproduction in heavy-ion collisions at LHC energies.

ACKNOWLEDGMENTS

This work is supported in part by National Key R & D Program of China under grant No. 2018YFA0404204, the NSFC (China) grant Nos. 11747086 and 12150013. Z. M. is funded by China Postdoctoral Science Foundation under grant No. 2021M692729.

Appendix A: Wavefunctions and long-distance matrix elements of heavy quarkonium

We list here, for the reader's convenience and for completeness, a detailed account of the involved wavefunctions and MEs. In the NRQCD, the Fock state structure of heavy quarkonium is [47]

$$\begin{aligned} |^{2S+1}L_J\rangle = & \mathcal{O}(1)|^{2S+1}L_J^{(1)}\rangle \\ & + \mathcal{O}(v)|^{2S+1}(L\pm 1)_{J'}^{(8)}g\rangle \\ & + \mathcal{O}(v^2)|^{2(S\pm 1)+1}(L\pm 1)_{J'}^{(8)}g\rangle \\ & + \mathcal{O}(v^2)|^{2S+1}L_J^{(1,8)}gg\rangle \\ & + \dots, \end{aligned} \quad (\text{A1})$$

where v is the relative velocity of the heavy quarks.

The wavefunctions of the charmonium (J/ψ , $\psi(2S)$, η_c , h_c , and χ_{cJ}) can be presented as follows,

$$\begin{aligned} |J/\psi\rangle = & \langle\mathcal{O}^{J/\psi}[^3S_1^{(1)}]\rangle|Q\bar{Q}[^3S_1^{(1)}]\rangle \\ & + \langle\mathcal{O}^{J/\psi}[^1S_0^{(8)}]\rangle|Q\bar{Q}[^1S_0^{(8)}]g\rangle \\ & + \langle\mathcal{O}^{J/\psi}[^3S_1^{(8)}]\rangle|Q\bar{Q}[^3S_1^{(8)}]gg\rangle \\ & + \sum_{J'}\langle\mathcal{O}^{J/\psi}[^3P_{J'}^{(8)}]\rangle|Q\bar{Q}[^3P_{J'}^{(8)}]g\rangle \\ & + \dots, \end{aligned} \quad (\text{A2})$$

$$\begin{aligned} |\psi(2S)\rangle = & \langle\mathcal{O}^{\psi(2S)}[^3S_1^{(1)}]\rangle|Q\bar{Q}[^3S_1^{(1)}]\rangle \\ & + \langle\mathcal{O}^{\psi(2S)}[^1S_0^{(8)}]\rangle|Q\bar{Q}[^1S_0^{(8)}]g\rangle \\ & + \langle\mathcal{O}^{\psi(2S)}[^3S_1^{(8)}]\rangle|Q\bar{Q}[^3S_1^{(8)}]gg\rangle \\ & + \sum_{J'}\langle\mathcal{O}^{\psi(2S)}[^3P_{J'}^{(8)}]\rangle|Q\bar{Q}[^3P_{J'}^{(8)}]g\rangle \\ & + \dots, \end{aligned} \quad (\text{A3})$$

$$\begin{aligned} |\chi_{cJ}\rangle = & \langle\mathcal{O}^{\chi_{cJ}}[^3P_J^{(1)}]\rangle|Q\bar{Q}[^3P_J^{(1)}]\rangle \\ & + \langle\mathcal{O}^{\chi_{cJ}}[^1S_0^{(8)}]\rangle|Q\bar{Q}[^1S_0^{(8)}]g\rangle \\ & + \langle\mathcal{O}^{\chi_{cJ}}[^3S_1^{(8)}]\rangle|Q\bar{Q}[^3S_1^{(8)}]g\rangle \\ & + \langle\mathcal{O}^{\chi_{cJ}}[^1P_1^{(8)}]\rangle|Q\bar{Q}[^1P_1^{(8)}]g\rangle \\ & + \langle\mathcal{O}^{\chi_{cJ}}[^3P_J^{(8)}]\rangle|Q\bar{Q}[^3P_J^{(8)}]gg\rangle \\ & + \langle\mathcal{O}^{\chi_{cJ}}[^3D_J^{(8)}]\rangle|Q\bar{Q}[^3D_J^{(8)}]g\rangle \\ & + \dots, \end{aligned} \quad (\text{A4})$$

$$\begin{aligned} |\eta_c\rangle = & \langle\mathcal{O}^{\eta_c}[^1S_0^{(1)}]\rangle|Q\bar{Q}[^1S_0^{(1)}]\rangle \\ & + \langle\mathcal{O}^{\eta_c}[^1S_0^{(8)}]\rangle|Q\bar{Q}[^1S_0^{(8)}]g\rangle \\ & + \langle\mathcal{O}^{\eta_c}[^3S_1^{(8)}]\rangle|Q\bar{Q}[^3S_1^{(8)}]g\rangle \\ & + \langle\mathcal{O}^{\eta_c}[^1P_1^{(8)}]\rangle|Q\bar{Q}[^1P_1^{(8)}]g\rangle \\ & + \dots, \end{aligned} \quad (\text{A5})$$

$$\begin{aligned} |h_c\rangle = & \langle\mathcal{O}^{h_c}[^1P_1^{(1)}]\rangle|Q\bar{Q}[^1P_1^{(1)}]g\rangle \\ & + \langle\mathcal{O}^{h_c}[^1S_0^{(8)}]\rangle|Q\bar{Q}[^1S_0^{(8)}]g\rangle \\ & + \dots, \end{aligned} \quad (\text{A6})$$

where $\langle\mathcal{O}^H[^{2S+1}L_J^{[1,8]}]\rangle$ is the MEs for the charmonium [65–70], its specific expressions are given by

$$\begin{aligned} \langle\mathcal{O}^{J/\psi}[^3S_1^{(1)}]\rangle &= 1.2 \text{ GeV}^3, \\ \langle\mathcal{O}^{J/\psi}[^1S_0^{(8)}]\rangle &= (0.0180 \pm 0.0087) \text{ GeV}^3, \\ \langle\mathcal{O}^{J/\psi}[^3S_1^{(8)}]\rangle &= (0.0013 \pm 0.0013) \text{ GeV}^3, \\ \langle\mathcal{O}^{J/\psi}[^3P_0^{(8)}]\rangle &= (0.0180 \pm 0.0087)m_c^2 \text{ GeV}^3, \\ \langle\mathcal{O}^{J/\psi}[^3P_1^{(8)}]\rangle &= 3 \times \langle\mathcal{O}^{J/\psi}[^3P_0^{(8)}]\rangle, \end{aligned}$$

$$\langle \mathcal{O}^{J/\psi} [{}^3P_2^{(8)}] \rangle = 5 \times \langle \mathcal{O}^{J/\psi} [{}^3P_0^{(8)}] \rangle, \quad (\text{A7})$$

$$\begin{aligned} \langle \mathcal{O}^{\psi(2S)} [{}^3S_1^{(1)}] \rangle &= 0.76 \text{ GeV}^3, \\ \langle \mathcal{O}^{\psi(2S)} [{}^1S_0^{(8)}] \rangle &= (0.0080 \pm 0.0067) \text{ GeV}^3, \\ \langle \mathcal{O}^{\psi(2S)} [{}^3S_1^{(8)}] \rangle &= (0.00330 \pm 0.00021) \text{ GeV}^3, \\ \langle \mathcal{O}^{\psi(2S)} [{}^3P_0^{(8)}] \rangle &= (0.0080 \pm 0.0067) m_c^2 \text{ GeV}^3, \\ \langle \mathcal{O}^{\psi(2S)} [{}^3P_1^{(8)}] \rangle &= 3 \times \langle \mathcal{O}^{\psi(2S)} [{}^3P_0^{(8)}] \rangle, \\ \langle \mathcal{O}^{\psi(2S)} [{}^3P_2^{(8)}] \rangle &= 5 \times \langle \mathcal{O}^{\psi(2S)} [{}^3P_0^{(8)}] \rangle, \end{aligned} \quad (\text{A8})$$

$$\begin{aligned} \langle \mathcal{O}^{\chi_{c0}} [{}^3P_0^{(1)}] \rangle &= 0.054 m_c^2 \text{ GeV}^3, \\ \langle \mathcal{O}^{\chi_{c0}} [{}^3S_1^{(8)}] \rangle &= (0.00187 \pm 0.00025) \text{ GeV}^3, \\ \langle \mathcal{O}^{\chi_{c1}} [{}^3P_1^{(1)}] \rangle &= 3 \times \langle \mathcal{O}^{\chi_{c0}} [{}^3P_0^{(1)}] \rangle, \\ \langle \mathcal{O}^{\chi_{c1}} [{}^3S_1^{(8)}] \rangle &= 3 \times \langle \mathcal{O}^{\chi_{c0}} [{}^3S_1^{(8)}] \rangle, \\ \langle \mathcal{O}^{\chi_{c2}} [{}^3P_1^{(1)}] \rangle &= 5 \times \langle \mathcal{O}^{\chi_{c0}} [{}^3P_0^{(1)}] \rangle, \\ \langle \mathcal{O}^{\chi_{c2}} [{}^3S_1^{(8)}] \rangle &= 5 \times \langle \mathcal{O}^{\chi_{c0}} [{}^3S_1^{(8)}] \rangle, \end{aligned} \quad (\text{A9})$$

$$\begin{aligned} \langle \mathcal{O}^{\eta_c} [{}^1S_0^{(1)}] \rangle &= \frac{1}{3} \times 1.2 \text{ GeV}^3, \\ \langle \mathcal{O}^{\eta_c} [{}^1S_0^{(8)}] \rangle &= \frac{1}{3} \times (0.0013 \pm 0.0013) \text{ GeV}^3, \\ \langle \mathcal{O}^{\eta_c} [{}^3S_1^{(8)}] \rangle &= (0.0180 \pm 0.0087) \text{ GeV}^3, \\ \langle \mathcal{O}^{\eta_c} [{}^1P_1^{(8)}] \rangle &= 3m_c^2 \langle \mathcal{O}^{\eta_c} [{}^3S_1^{(8)}] \rangle, \\ \langle \mathcal{O}^{h_c} [{}^1P_1^{(1)}] \rangle &= 3 \times 0.54 m_c^2 \text{ GeV}^3, \\ \langle \mathcal{O}^{h_c} [{}^1S_0^{(8)}] \rangle &= 3 \times (0.00187 \pm 0.00025) \text{ GeV}^3, \end{aligned} \quad (\text{A10})$$

The wavefunctions of the bottomonium ($\Upsilon(ns)$, χ_{bJ} , η_b , and h_b) are

$$\begin{aligned} |\Upsilon(ns)\rangle &= \langle \mathcal{O}^{\Upsilon(ns)} [{}^3S_1^{(1)}] | Q\bar{Q} [{}^3S_1^{(1)}] \rangle \\ &+ \langle \mathcal{O}^{\Upsilon(ns)} [{}^1S_0^{(8)}] | Q\bar{Q} [{}^1S_0^{(8)}] g \rangle \\ &+ \langle \mathcal{O}^{\Upsilon(ns)} [{}^3S_1^{(8)}] | Q\bar{Q} [{}^3S_1^{(8)}] gg \rangle \\ &+ \sum_{J'} \langle \mathcal{O}^{\Upsilon(ns)} [{}^3P_{J'}^{(8)}] | Q\bar{Q} [{}^3P_{J'}^{(8)}] g \rangle \\ &+ \dots, \end{aligned} \quad (\text{A11})$$

$$\begin{aligned} |\chi_{bJ}\rangle &= \langle \mathcal{O}^{\chi_{bJ}} [{}^3P_J^{(1)}] | Q\bar{Q} [{}^3P_J^{(1)}] \rangle \\ &+ \langle \mathcal{O}^{\chi_{bJ}} [{}^1S_0^{(8)}] | Q\bar{Q} [{}^1S_0^{(8)}] g \rangle \\ &+ \langle \mathcal{O}^{\chi_{bJ}} [{}^3S_1^{(8)}] | Q\bar{Q} [{}^3S_1^{(8)}] g \rangle \\ &+ \langle \mathcal{O}^{\chi_{bJ}} [{}^1P_1^{(8)}] | Q\bar{Q} [{}^1P_1^{(8)}] g \rangle \\ &+ \langle \mathcal{O}^{\chi_{bJ}} [{}^3P_J^{(8)}] | Q\bar{Q} [{}^3P_J^{(8)}] gg \rangle \\ &+ \langle \mathcal{O}^{\chi_{bJ}} [{}^3D_J^{(8)}] | Q\bar{Q} [{}^3D_J^{(8)}] g \rangle \\ &+ \dots, \end{aligned} \quad (\text{A12})$$

$$\begin{aligned} |\eta_b\rangle &= \langle \mathcal{O}^{\eta_b} [{}^1S_0^{(1)}] | Q\bar{Q} [{}^1S_0^{(1)}] \rangle \\ &+ \langle \mathcal{O}^{\eta_b} [{}^1S_0^{(8)}] | Q\bar{Q} [{}^1S_0^{(8)}] g \rangle \\ &+ \langle \mathcal{O}^{\eta_b} [{}^3S_1^{(8)}] | Q\bar{Q} [{}^3S_1^{(8)}] g \rangle \\ &+ \langle \mathcal{O}^{\eta_b} [{}^1P_1^{(8)}] | Q\bar{Q} [{}^1P_1^{(8)}] g \rangle \\ &+ \dots, \end{aligned} \quad (\text{A13})$$

$$\begin{aligned} |h_b\rangle &= \langle \mathcal{O}^{h_b} [{}^1P_1^{(1)}] | Q\bar{Q} [{}^1P_1^{(1)}] g \rangle \\ &+ \langle \mathcal{O}^{h_b} [{}^1S_0^{(8)}] | Q\bar{Q} [{}^1S_0^{(8)}] g \rangle \\ &+ \dots, \end{aligned} \quad (\text{A14})$$

where the MEs for the bottomonium [70–73] are,

$$\begin{aligned} \langle \mathcal{O}^{\Upsilon(1S)} [{}^3S_1^{(1)}] \rangle &= 10.9 \text{ GeV}^3, \\ \langle \mathcal{O}^{\Upsilon(1S)} [{}^1S_0^{(8)}] \rangle &= (0.0121 \pm 0.0400) \text{ GeV}^3, \\ \langle \mathcal{O}^{\Upsilon(1S)} [{}^3S_1^{(8)}] \rangle &= (0.0477 \pm 0.0334) \text{ GeV}^3, \\ \langle \mathcal{O}^{\Upsilon(1S)} [{}^3P_0^{(8)}] \rangle &= 5m_b^2 \langle \mathcal{O}^{\Upsilon(1S)} [{}^1S_0^{(8)}] \rangle, \end{aligned} \quad (\text{A15})$$

$$\begin{aligned} \langle \mathcal{O}^{\Upsilon(2S)} [{}^3S_1^{(1)}] \rangle &= 4.5 \text{ GeV}^3, \\ \langle \mathcal{O}^{\Upsilon(2S)} [{}^1S_0^{(8)}] \rangle &= (-0.0067 \pm 0.0084) \text{ GeV}^3, \\ \langle \mathcal{O}^{\Upsilon(2S)} [{}^3S_1^{(8)}] \rangle &= (0.0224 \pm 0.0200) \text{ GeV}^3, \\ \langle \mathcal{O}^{\Upsilon(2S)} [{}^3P_0^{(8)}] \rangle &= 5m_b^2 \langle \mathcal{O}^{\Upsilon(2S)} [{}^1S_0^{(8)}] \rangle, \end{aligned} \quad (\text{A16})$$

$$\begin{aligned} \langle \mathcal{O}^{\Upsilon(3S)} [{}^3S_1^{(1)}] \rangle &= 4.3 \text{ GeV}^3, \\ \langle \mathcal{O}^{\Upsilon(3S)} [{}^1S_0^{(8)}] \rangle &= (0.0002 \pm 0.0062) \text{ GeV}^3, \\ \langle \mathcal{O}^{\Upsilon(3S)} [{}^3S_1^{(8)}] \rangle &= (0.0513 \pm 0.0085) \text{ GeV}^3, \\ \langle \mathcal{O}^{\Upsilon(3S)} [{}^3P_0^{(8)}] \rangle &= 5m_b^2 \langle \mathcal{O}^{\Upsilon(3S)} [{}^1S_0^{(8)}] \rangle, \end{aligned} \quad (\text{A17})$$

$$\begin{aligned} \langle \mathcal{O}^{\chi_{b0}(1P)} [{}^3P_0^{(1)}] \rangle &= 0.1 m_b^2 \text{ GeV}^3, \\ \langle \mathcal{O}^{\chi_{b0}(1P)} [{}^3S_1^{(8)}] \rangle &= 0.1008 \text{ GeV}^3, \\ \langle \mathcal{O}^{\chi_{b0}(2P)} [{}^3P_0^{(1)}] \rangle &= 0.036 m_b^2 \text{ GeV}^3, \\ \langle \mathcal{O}^{\chi_{b0}(2P)} [{}^3S_1^{(8)}] \rangle &= 0.0324 \text{ GeV}^3, \\ \langle \mathcal{O}^{\chi_{b1}(1P)} [{}^3P_1^{(1)}] \rangle &= 6.1 \text{ GeV}^5, \\ \langle \mathcal{O}^{\chi_{b1}(1P)} [{}^3S_1^{(8)}] \rangle &= 0.43 \text{ GeV}^3, \\ \langle \mathcal{O}^{\chi_{b1}(2P)} [{}^3P_1^{(1)}] \rangle &= 7.1 m_b^2 \text{ GeV}^3, \\ \langle \mathcal{O}^{\chi_{b1}(2P)} [{}^3S_1^{(8)}] \rangle &= 0.52 \text{ GeV}^3, \\ \langle \mathcal{O}^{\chi_{b1}(3P)} [{}^3P_1^{(1)}] \rangle &= 7.7 m_b^2 \text{ GeV}^3, \end{aligned} \quad (\text{A18})$$

$$\begin{aligned} \langle \mathcal{O}^{\eta_b(ns)} [{}^1S_0^{(1)}] \rangle &= \frac{1}{3} \times \langle \mathcal{O}^{\Upsilon(ns)} [{}^3S_1^{(1)}] \rangle, \\ \langle \mathcal{O}^{\eta_b(ns)} [{}^1S_0^{(8)}] \rangle &= \frac{1}{3} \times \langle \mathcal{O}^{\Upsilon(ns)} [{}^3S_1^{(8)}] \rangle, \\ \langle \mathcal{O}^{\eta_b(ns)} [{}^3S_1^{(8)}] \rangle &= \langle \mathcal{O}^{\Upsilon(ns)} [{}^1S_0^{(8)}] \rangle, \end{aligned}$$

$$\langle \mathcal{O}^{\eta_b(nS)}[{}^1P_1^{(8)}] \rangle = 3 \times \langle \mathcal{O}^{\Upsilon(nS)}[{}^3P_0^{(8)}] \rangle, \quad (\text{A19})$$

$$\begin{aligned} \langle \mathcal{O}^{h_b(nP)}[{}^1P_1^{(1)}] \rangle &= 3 \times \langle \mathcal{O}^{\chi_{b0}(nP)}[{}^3P_0^{(1)}] \rangle, \\ \langle \mathcal{O}^{h_b(nP)}[{}^1S_0^{(8)}] \rangle &= 3 \times \langle \mathcal{O}^{\chi_{b0}(nP)}[{}^3S_1^{(8)}] \rangle. \end{aligned} \quad (\text{A20})$$

Appendix B: Full kinematical relations

We give here a detailed treatment of the partonic kinematics which is matched with the exact treatment.

The energy and momentum in αb CM frame read

$$\begin{aligned} E_\alpha &= \frac{(s_{\alpha b} + m_\alpha^2)}{2\sqrt{s_{\alpha b}}}, \\ E_b &= \frac{(s_{\alpha b} - m_\alpha^2)}{2\sqrt{s_{\alpha b}}}, \\ p_{\text{CM}} &= \frac{(s_{\alpha b} - m_\alpha^2)}{2\sqrt{s_{\alpha b}}}, \end{aligned} \quad (\text{B1})$$

where the specific expressions of $s_{\alpha b}$ for each photon emission processes are

$$\begin{aligned} s_{\alpha b}|\text{coh.} &= m_A^2 + \frac{x_b}{N_B}(s - m_A^2 - m_B^2), \\ s_{\alpha b}|\text{OIC.} &= m_p^2 + \frac{x_b}{N_A N_B}(s - m_A^2 - m_B^2), \\ s_{\alpha b}|\text{UIC.} &= m_a^2 + \frac{x_a x_b}{N_A N_B}(s - m_A^2 - m_B^2), \end{aligned} \quad (\text{B2})$$

where $s = (p_A + p_B)^2 = (N_A + N_B)^2 s_{NN}/4$ is the energy square of AB CM frame.

While the energy and momentum in $\gamma^* b$ CM frame are

$$\begin{aligned} \hat{E}_\gamma &= \frac{(\hat{s} - Q^2)}{2\sqrt{\hat{s}}}, \\ \hat{E}_H &= \frac{(\hat{s} + M_H^2)}{2\sqrt{\hat{s}}}, \\ \hat{p}_{\text{CM}} &= \frac{(\hat{s} + Q^2)}{2\sqrt{\hat{s}}}, \end{aligned}$$

$$\hat{p}'_{\text{CM}} = \frac{(\hat{s} - M_H^2)}{2\sqrt{\hat{s}}}, \quad (\text{B3})$$

The Mandelstam variables involved in the case of direct photoproduction processes are

$$\begin{aligned} \hat{s} &= (q + p_b)^2 = y(s_{\alpha b} - m_\alpha^2) - Q^2, \\ \hat{t} &= (q - p_H)^2 = -(1 - z)(\hat{s} + Q^2), \\ \hat{u} &= (p_b - p_H)^2 = M_H^2 - z(\hat{s} + Q^2), \end{aligned} \quad (\text{B4})$$

while those in the case of resolved photoproduction processes can be presented as

$$\begin{aligned} \hat{s}^* &= (p_{a'} + p_b)^2 = yz_{a'}(s_{\alpha b} - m_\alpha^2), \\ \hat{t}^* &= (p_{a'} - p_H)^2 = -(1 - z)\hat{s}^*, \\ \hat{u}^* &= (p_b - p_H)^2 = M_H^2 - z\hat{s}^*. \end{aligned} \quad (\text{B5})$$

We summarize the kinematical boundaries in Table V for y and Q^2 distributions; while those for p_T distribution are summarized into Table VI.

Finally, we give here the complete expressions of the Jacobian determinant \mathcal{J} for each distribution. In the case of the Q^2 and y distributions, we have

$$\mathcal{J} = \frac{2r^2 |\mathbf{p}_b|}{E_{\alpha'} E_b} = \frac{2r^2}{\sqrt{(r^2 + m_\alpha^2)}}. \quad (\text{B6})$$

In the case of the p_T distribution, the Jacobian determinant \mathcal{J} should be written as

$$\mathcal{J} = \frac{(\hat{s}^{3/2} + Q^2 \sqrt{\hat{s}})}{y(s_{\alpha b} - m_\alpha^2)(\sqrt{\hat{s}} - \cosh y_r m_T)}, \quad (\text{B7})$$

for coherent-direct process. And the relations between Eq. (B7) and the rest cases are: $\mathcal{J}_{\text{incoh.dir.}} = \mathcal{J}/x_a$, $\mathcal{J}_{\text{coh.res.}} = \mathcal{J}/x_b$, and $\mathcal{J}_{\text{incoh.res.}} = \mathcal{J}/x_a x_b$. In the case of fragmentation processes, $\mathcal{J} = (\hat{s} + Q^2)/\cosh y_r \sqrt{\hat{s}}$.

-
- [1] V. P. Goncalves and M. V. T. Machado, Mod. Phys. Lett. A **19**, 2525-2539 (2004); C.A. Bertulani, S.R. Klein and J. Nystrand, Nucl. Rev. Part. Sci. **55**, 271 (2005); A. J. Baltz, G. Baur, D. d'Enterria, *et al.* Phys. Rept. **458**, 1-171 (2008).
 - [2] G. Baur, K. Hencken, D. Trautmann, S. Sadovsky and Y. Kharlov, Phys. Rept. **364**, 359-450 (2002).
 - [3] K. Akiba *et al.* [LHC Forward Physics Working Group], J. Phys. G **43**, 110201 (2016).
 - [4] Z. L. Ma and J. Q. Zhu, Phys. Rev. D **97**, no.5, 054030 (2018).
 - [5] Z. L. Ma, Z. Lu, J. Q. Zhu and L. Zhang, Phys. Rev. D **104**, no.7, 074023 (2021).
 - [6] Z. L. Ma, Z. Lu and L. Zhang, Nucl. Phys. B **974**, 115645 (2022).
 - [7] V. P. Goncalves and C. A. Bertulani, Phys. Rev. C **65**, 054905 (2002).
 - [8] V. P. Goncalves and M. V. T. Machado, Eur. Phys. J. C **40**, 519-529 (2005); Phys. Rev. C **73**, 044902 (2006); Phys. Rev. D **77**, 014037 (2008); Phys. Rev. C **84**, 011902 (2011).
 - [9] A. Manohar, P. Nason, G. P. Salam and G. Zanderighi, Phys. Rev. Lett. **117**, no.24, 242002 (2016).
 - [10] S. R. Klein, J. Nystrand and R. Vogt, Phys. Rev. C **66**, 044906 (2002); S. R. Klein, Nucl. Phys. A **967**, 249-256 (2017).
 - [11] C. A. Salgado, J. Alvarez-Muniz, F. Arleo, N. Armesto, M. Botje, M. Cacciari, J. Campbell, C. Carli, B. Cole

TABLE V: The kinematical boundaries of Q^2 , y distributions. $\hat{s}_{\min} = \hat{s}_{\min}^* = (m_T + p_{T\min})^2$, $p_T^2 = \hat{t}(\hat{s}\hat{u} + Q^2 M_H^2)/(\hat{s} + Q^2)^2$.

Variables	Coherent direct	UIC direct	Coherent resolved	UIC resolved
z_{\min}		$[(M_H^2 + \hat{s}) - \sqrt{(\hat{s} - M_H^2)^2 - 4p_{T\min}^2 \hat{s}}]/(2\hat{s})$		
z_{\max}		$[(M_H^2 + \hat{s}) + \sqrt{(\hat{s} - M_H^2)^2 - 4p_{T\min}^2 \hat{s}}]/(2\hat{s})$		
\hat{t}_{\min}	$-(1 - z_{\min})(\hat{s} + Q^2)$		$-(1 - z_{\min})\hat{s}^*$	
\hat{t}_{\max}	$-(1 - z_{\max})(\hat{s} + Q^2)$		$-(1 - z_{\max})\hat{s}^*$	
$z_{a'\min}$	\	\	$N_A \hat{s}_{\min}^*/[yx_b(s - m_A^2 - m_B^2)]$	$\hat{s}_{\min}^*/(yx_a x_b s_{NN})$
$z_{a'\max}$	\	\	1	1
$x_{b\min}$	$N_A(\hat{s}_{\min} + Q^2)/[y(s - m_A^2 - m_B^2)]$	$(\hat{s}_{\min} + Q^2)/(yx_a s_{NN})$	$N_A \hat{s}_{\min}^*/[y(s - m_A^2 - m_B^2)]$	$\hat{s}_{\min}^*/(yx_a s_{NN})$
$x_{b\max}$		1		
$x_{a\min}$	\	$(\hat{s}_{\min} + Q^2)/(ys_{NN})$	\	$\hat{s}_{\min}^*/(ys_{NN})$
$x_{a\max}$	\	1	\	1
y_{\min}	$N_A(\hat{s}_{\min} + Q^2)/(s - m_A^2 - m_B^2)$	$(\hat{s}_{\min} + Q^2)/s_{NN}$	$N_A \hat{s}_{\min}^*/(s - m_A^2 - m_B^2)$	\hat{s}_{\min}^*/s_{NN}
y_{\max}		$[\sqrt{Q^2(4m_\alpha^2 + Q^2)} - Q^2]/(2m_\alpha^2)$		
Q_{\min}^2	$Q_{\min}^2 = -2m_\alpha^2 + [(s_{\alpha b} + m_\alpha^2)(s_{\alpha b} - \hat{s} + m_\alpha^2) - (s_{\alpha b} - m_\alpha^2)\sqrt{(s_{\alpha b} - \hat{s} + m_\alpha^2)^2 - 4s_{\alpha b}m_\alpha^2}]/(2s_{\alpha b})$			
Q_{\max}^2	$Q_{\min}^2 = -2m_\alpha^2 + [(s_{\alpha b} + m_\alpha^2)(s_{\alpha b} - \hat{s} + m_\alpha^2) + (s_{\alpha b} - m_\alpha^2)\sqrt{(s_{\alpha b} - \hat{s} + m_\alpha^2)^2 - 4s_{\alpha b}m_\alpha^2}]/(2s_{\alpha b})$			

TABLE VI: Same as Table V but for p_T distribution. $x_1 = \hat{s}/s_{\alpha b}$, $\tau = M_H^2/\hat{s}_{\max}$, $\tau' = m_d^2/\hat{s}_{\max}$, and $z_{a'\max} = 1/(1 + Q^2/4p_T^2)$. The other kinematical boundaries are the same as Table V, we are not list it here.

Variables	Coherent direct	UIC direct	Coherent resolved	UIC resolved
Q_{\min}^2		$x_1^2 m_\alpha^2/(1 - x_1)$		
Q_{\max}^2	$1/R_\alpha^2$	$(1 - x_1)s_{NN}$	$1/R_\alpha^2$	$(1 - x_1)s_{NN}$
$ y_{r\max} $	$\ln[(\hat{s}_{\max} + M_H^2 + \sqrt{(\hat{s}_{\max} - M_H^2)^2 - 4p_T^2 \hat{s}_{\max}})/(\hat{s}_{\max} + M_H^2 - \sqrt{(\hat{s}_{\max} - M_H^2)^2 - 4p_T^2 \hat{s}_{\max}})]^{1/2}$			
$p_{T\min}$		M_H		
$p_{T\max}$	$\sqrt{\hat{s}_{\max}} [(1 - \tau)^2 + (1 - \tau')^2 - 2\tau\tau' - 4\tau \sinh^2 y_r - 1]^{\frac{1}{2}}/(2 \cosh y_r)$			

and D. D'Enterria, *et al.* J. Phys. G **39**, 015010 (2012).

- [12] E. Fermi, Z. Phys. **29**, 315-327 (1924).
[13] C. F. von Weizsacker, Z. Phys. **88**, 612-625 (1934).
[14] E. J. Williams, Phys. Rev. **45**, 729 (1934).
[15] M. Drees and D. Zeppenfeld, Phys. Rev. D **39**, 2536 (1989).
[16] J. Q. Zhu, Z. L. Ma, C. Y. Shi and Y. D. Li, Phys. Rev. C **92**, no.5, 054907 (2015).
[17] G. M. Yu, Y. C. Yu, Y. D. Li and J. S. Wang, Nucl. Phys. B **917**, 234-240 (2017).
[18] Y. P. Fu and Y. D. Li, Phys. Rev. C **84**, 044906 (2011).
[19] Y. P. Fu and Y. D. Li, Nucl. Phys. A **865**, 76-82 (2011).
[20] G. M. Yu and Y. D. Li, Phys. Rev. C **91**, no.4, 044908 (2015).
[21] G. M. Yu, Y. B. Cai, Y. D. Li and J. S. Wang, Phys. Rev. C **95**, no.1, 014905 (2017).
[22] B. A. Kniehl, Phys. Lett. B **254**, 267-273 (1991).
[23] Y. P. Fu and Y. D. Li, Chin. Phys. C **36**, 721 (2012); Chin. Phys. Lett. **29**, 102501 (2012). J. Q. Zhu and Y. D. Li, Chin. Phys. Lett. **29**, 081301 (2012). G. M. Yu and Y. D. Li, Chin. Phys. Lett. **31**, 011202 (2014); Chin. Phys. Lett. **30**, 011201 (2013).
[24] J. Q. Zhu, Z. L. Ma, C. Y. Shi and Y. D. Li, Nucl. Phys. B **900**, 431-445 (2015).

- [25] J. Nystrand, Nucl. Phys. A **752**, 470-479 (2005); Nucl. Phys. A **787**, 29-36 (2007).
- [26] S. Frixione, M. L. Mangano, P. Nason and G. Ridolfi, Phys. Lett. B **319**, 339-345 (1993).
- [27] B. A. Kniehl and L. Zwierner, Nucl. Phys. B **621**, 337-358 (2002).
- [28] M. Drees, J. R. Ellis and D. Zeppenfeld, Phys. Lett. B **223**, 454-460 (1989).
- [29] A. Winther, K. Alder, Nucl. Phys. A **319**, 518 (1979); C. A. Bertulani, G. Baur, Nucl. Phys. A **442**, 739 (1985); C. A. Bertulani, G. Baur, Nucl. Phys. A **458**, 725 (1986); E. Papageorgiu, Phys. Lett. B **250**, 155 (1990).
- [30] Y. Yang, S. Cai, Y. Cai and W. Xiang, Nucl. Phys. A **990**, 17-28 (2019).
- [31] J. Wu, Y. Cai and W. Xiang, Phys. Rev. C **104**, no.1, 015204 (2021).
- [32] G. Baur, K. Hencken and D. Trautmann, J. Phys. G **24**, 1657-1692 (1998).
- [33] V. P. Gonçalves and R. Palota da Silva, Phys. Rev. D **101**, no.3, 034025 (2020).
- [34] Y. P. Xie and V. P. Goncalves, Eur. Phys. J. C **81**, no.7, 645 (2021).
- [35] V. P. Gonçalves, F. S. Navarra and D. Spiering, Phys. Lett. B **791**, 299-304 (2019).
- [36] V. P. Gonçalves and M. M. Jaime, Eur. Phys. J. C **78**, no.9, 693 (2018).
- [37] V. P. Goncalves and M. M. Machado, Eur. Phys. J. A **50**, 72 (2014).
- [38] L. Jenkovszky, V. Libov and M. V. T. Machado, Phys. Lett. B **824**, 136836 (2022).
- [39] F. Kopp and M. V. T. Machado, Phys. Rev. D **98**, 014010 (2018).
- [40] V. P. Gonçalves, M. V. T. Machado, B. D. Moreira, F. S. Navarra and G. S. dos Santos, Phys. Rev. D **96**, no.9, 094027 (2017).
- [41] G. Sampaio dos Santos and M. V. T. Machado, J. Phys. G **42**, no.10, 105001 (2015).
- [42] A. J. Baltz, S. R. Klein and J. Nystrand, Phys. Rev. Lett. **89**, 012301 (2002).
- [43] S. R. Klein and J. Nystrand, Phys. Rev. Lett. **92**, 142003 (2004); Phys. Rev. C **60**, 014903 (1999).
- [44] S. R. Klein and Y. P. Xie, Phys. Rev. C **100**, no.2, 024620 (2019); M. Lomnitz and S. Klein, Phys. Rev. C **99**, no.1, 015203 (2019).
- [45] S. R. Klein, J. Nystrand, J. Seger, Y. Gorbunov and J. Butterworth, Comput. Phys. Commun. **212**, 258-268 (2017).
- [46] S. Fleming and T. Mehen, Phys. Rev. D **57**, 1846-1857 (1998).
- [47] G. T. Bodwin, E. Braaten and G. P. Lepage, Phys. Rev. D **51**, 1125-1171 (1995) [erratum: Phys. Rev. D **55**, 5853 (1997)].
- [48] K. J. Eskola, P. Paakinen, H. Paukkunen and C. A. Salgado, Eur. Phys. J. C **77**, no.3, 163 (2017).
- [49] S. Bailey, T. Cridge, L. A. Harland-Lang, A. D. Martin and R. S. Thorne, Eur. Phys. J. C **81**, no.4, 341 (2021).
- [50] V. M. Budnev, I. F. Ginzburg, G. V. Meledin and V. G. Serbo, Phys. Rept. **15**, 181-281 (1975).
- [51] A. D. Martin and M. G. Ryskin, Eur. Phys. J. C **74**, 3040 (2014).
- [52] M. Dyndal, A. Glazov, M. Luszczak and R. Sadykov, Phys. Rev. D **99**, no.11, 114008 (2019).
- [53] M. Gluck, E. Reya and I. Schienbein, Phys. Rev. D **60**, 054019 (1999) [erratum: Phys. Rev. D **62**, 019902 (2000)].
- [54] M. Klasen, B. A. Kniehl, L. N. Mihaila and M. Steinhauser, Phys. Rev. D **68**, 034017 (2003); Phys. Rev. D **77**, 117501 (2008).
- [55] J. P. Ma, Phys. Rev. D **53**, 1185-1190 (1996).
- [56] Y. Q. Ma, J. W. Qiu and H. Zhang, Phys. Rev. D **89**, no.9, 094029 (2014); Phys. Rev. D **89**, no.9, 094030 (2014).
- [57] J. F. Owens, Rev. Mod. Phys. **59**, 465 (1987).
- [58] J.D. Jackson, Classical Electrodynamics, Wiley, New York, 1975.
- [59] M. Drees, R. M. Godbole, M. Nowakowski and S. D. Rindani, Phys. Rev. D **50**, 2335-2338 (1994).
- [60] S. J. Brodsky, T. Kinoshita and H. Terazawa, Phys. Rev. D **4**, 1532-1557 (1971).
- [61] K. A. Olive *et al.* [Particle Data Group], Chin. Phys. C **38**, 090001 (2014).
- [62] Z. L. Ma, J. Q. Zhu, C. Y. Shi and Y. D. Li, Chin. Phys. Lett. **32**, no.12, 121202 (2015).
- [63] K. Aamodt *et al.* [ALICE], Phys. Lett. B **704**, 442-455 (2011) [erratum: Phys. Lett. B **718**, 692-698 (2012)]; V. Khachatryan *et al.* [CMS], Phys. Rev. Lett. **114**, no.19, 191802 (2015).
- [64] V. Khachatryan *et al.* [CMS], Phys. Lett. B **749**, 14-34 (2015).
- [65] M. Butenschoen, Z. G. He and B. A. Kniehl, Phys. Rev. Lett. **114**, no.9, 092004 (2015).
- [66] H. Han, Y. Q. Ma, C. Meng, H. S. Shao and K. T. Chao, Phys. Rev. Lett. **114**, no.9, 092005 (2015).
- [67] H. F. Zhang, Z. Sun, W. L. Sang and R. Li, Phys. Rev. Lett. **114**, no.9, 092006 (2015).
- [68] J. X. Wang and H. F. Zhang, J. Phys. G **42**, no.2, 025004 (2015).
- [69] Z. G. He and B. A. Kniehl, Phys. Rev. Lett. **115**, no.2, 022002 (2015).
- [70] P. L. Cho and A. K. Leibovich, Phys. Rev. D **53**, 150-162 (1996); Phys. Rev. D **53**, 6203-6217 (1996).
- [71] R. Sharma and I. Vitev, Phys. Rev. C **87**, no.4, 044905 (2013).
- [72] E. Braaten, S. Fleming and A. K. Leibovich, Phys. Rev. D **63**, 094006 (2001).
- [73] J. L. Domenech and M. A. Sanchis-Lozano, Phys. Lett. B **476**, 65-72 (2000);